

West Chester University

## Digital Commons @ West Chester University

---

West Chester University Master's Theses

Masters Theses and Doctoral Projects

---

Fall 2022

### Evaluation of OASL and HERC5's role in the non-lytic clearance of influenza A virus from club cells

Steve Crisafulli  
sc964628@wcupa.edu

Follow this and additional works at: [https://digitalcommons.wcupa.edu/all\\_theses](https://digitalcommons.wcupa.edu/all_theses)



Part of the [Immunology of Infectious Disease Commons](#), [Molecular Biology Commons](#), and the [Virology Commons](#)

---

#### Recommended Citation

Crisafulli, Steve, "Evaluation of OASL and HERC5's role in the non-lytic clearance of influenza A virus from club cells" (2022). *West Chester University Master's Theses*. 267.  
[https://digitalcommons.wcupa.edu/all\\_theses/267](https://digitalcommons.wcupa.edu/all_theses/267)

This Thesis is brought to you for free and open access by the Masters Theses and Doctoral Projects at Digital Commons @ West Chester University. It has been accepted for inclusion in West Chester University Master's Theses by an authorized administrator of Digital Commons @ West Chester University. For more information, please contact [wcrestler@wcupa.edu](mailto:wcrestler@wcupa.edu).

Evaluation of OASL and HERC5's role in the non-lytic clearance of influenza A virus from club  
cells

A Thesis

Presented to the Faculty of the

Department of Biology

West Chester University

West Chester, Pennsylvania

In Partial Fulfillment of the Requirements for the

Degree of

Masters of Science

By

Steve Crisafulli

January 2023

© Copyright Crisafulli 2023

## Acknowledgements

I would like to express my greatest appreciation to everyone who helped and guided me throughout this project. Words cannot express my gratitude to my advisor, Dr. Ben Chambers, for his continuous support throughout my time at West Chester University. Dr. Chamber's teaching, advice, and encouragement were invaluable to the completion of this research and to my development as a researcher. I would further like to thank Dr. Jessica Sowa and Dr. Michael Rosario for their participation on my committee. Their time and feedback was greatly appreciated throughout the project. I would also like to thank Dr. Greg Turner. His guidance throughout my education at West Chester University was instrumental in setting and achieving my academic goals. I'd like to express my gratitude to Arkema Inc. for the generous financial aid provided to pursue this educational endeavor. Furthermore, I wish to thank my Arkema Inc. supervisor, Lisa Buckley, for her endless support of my professional and academic development. I'm extremely grateful to my parents, my brother, and my sister for their encouragement throughout my education and life in general. I'd also like to thank Allison Songstad and Jon Scholte for their constant feedback on my research efforts, particularly in preparation for my defense. Lastly, and certainly not least, I'd like to express my sincerest gratitude to my wife, Amanda Crisafulli, who is forever my greatest source of confidence, inspiration, and expertly-performed proof-reading. I could not have undertaken this journey without her. The completion of this project is just as much an accomplishment for those listed here, and more, as it is my own.

## Abstract

Influenza A virus (IAV) is a highly infectious pathogen responsible for causing severe respiratory illness and death in humans and animals worldwide. Due to highly effective strategies to negate host antiviral defenses, IAV leads to the death of nearly all infected cells. Furthermore, IAV induces high levels of genome-damaging oxidative stress within infected cells and suppresses the cellular mismatch repair (MMR) mechanism, thereby inhibiting expression of key antiviral genes, which further contributes to cell death. However, recent studies have demonstrated that a subset of respiratory epithelial cells, called club cells, are able to non-lytically clear IAV and continue to survive following direct infection. These cells are able to maintain genome integrity during IAV infection using MMR activity, thus allowing for sufficient expression of antiviral genes. We hypothesize that several of these antiviral genes are critical to the non-lytic clearance of IAV, particularly *HERC5* and *OSAL*. Through siRNA gene knockdown techniques, we have evaluated the impact of these genes on the non-lytic clearance mechanism of IAV-infected club cells.

## Table of Contents

Acknowledgements	ii
Abstract	iii
Table of Contents	iv
List of Tables and Figures	v
Introduction	1
Results	37
Discussion	67
References	78

## List of Tables and Figures

01. Figure 1: Diagram of an influenza A virus particle.....	Page 2
02. Table 1: IAV RNA segments, proteins, and functions.....	Page 3
03. Figure 2: Detection of IAV by PRRs triggers the innate immune response.....	Page 9
04. Figure 3: NS1 inhibits expression of interferon stimulated genes (ISGs).....	Page 14
05. Figure 4: H441 cells survive IAV infection.....	Page 18
06. Figure 5: OASL activates RIG-I through ubiquitin-like action.....	Page 28
07. Figure 6: OAS/RNase L pathway leads to viral dsRNA degradation.....	Page 30
08. Figure 7: HERC5 plays a critical role in the ISGylation of viral proteins.....	Page 33
09. Figure 8: Optimization of cell culture media.....	Page 39
10. Figure 9: Optimization of cell plating density.....	Page 41
11. Figure 10: Presence of hemagglutinin prevents pelletization of turkey red blood cells .....	Page 46
12. Figure 11: Hemagglutination assay (HA) results from PR8-Cre viruses grown in fertilized chicken eggs.....	Page 47
13. Figure 12: Hemagglutination assay (HA) results (with control included) from PR8-Cre viruses grown in fertilized chicken eggs.....	Page 48
14. Figure 13: Infection optimization.....	Page 49
15. Figure 14: siRNA control (negative and positive control) evaluation.....	Page 52
16. Figure 15a: siRNA control (negative and positive control) evaluation.....	Page 54
17. Figure 15b: siRNA control (negative and positive control) evaluation HA intensity pixel analysis.....	Page 55
18. Figure 16: siRNA confirmation (HERC5).....	Page 56

19. Figure 17: siRNA confirmation (OASL).....Page 58

20. Figure 18: Targeted gene evaluation (HERC5 and OASL).....Page 60

21. Figure 19a: Targeted gene evaluation (HERC5 and OASL).....Page 62

22. Figure 19b: Targeted gene evaluation (HERC5 and OASL) HA intensity pixel  
analysis.....Page 63

23. Figure 20a: Targeted gene evaluation over time (HERC5 and OASL).....Page 64

24. Figure 20b: Targeted gene evaluation over time (HERC5 and OASL) HA intensity pixel  
analysis.....Page 65

## Introduction

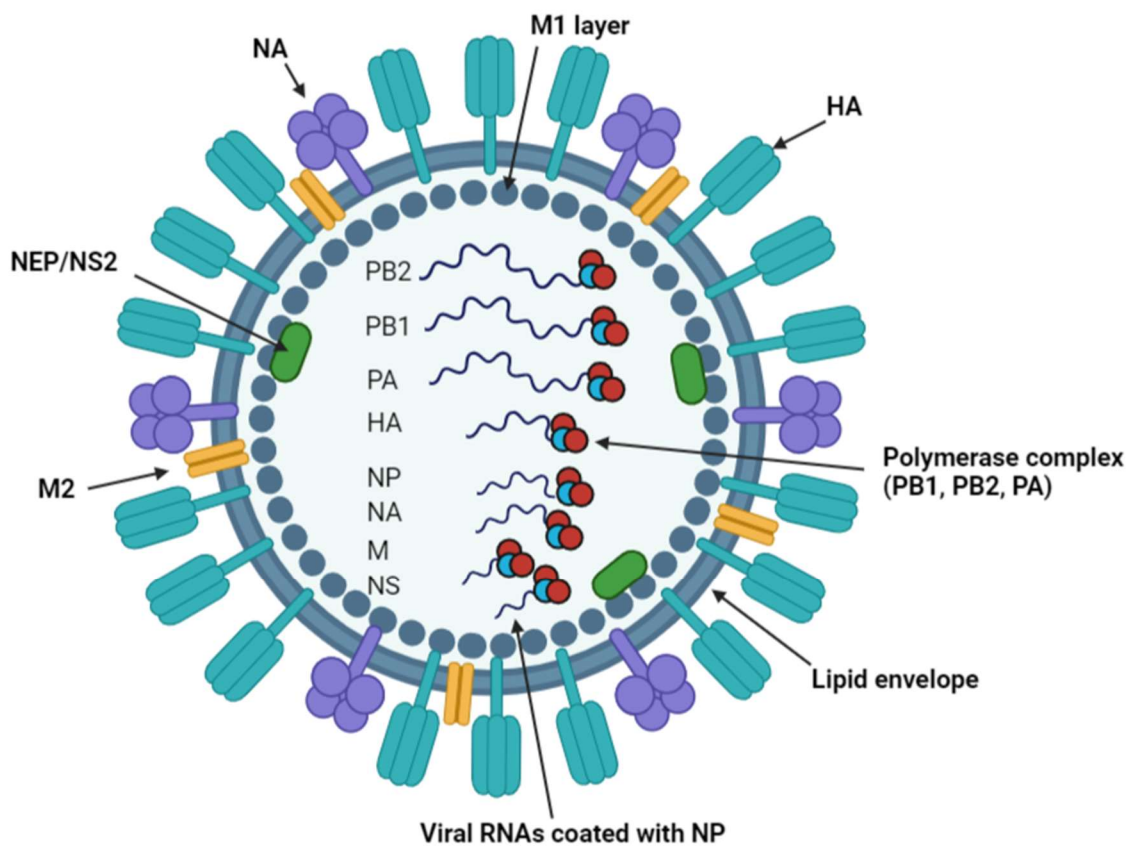
### *Influenza A virus is a highly infectious RNA virus*

Influenza A virus (IAV) is a globally-present pathogen that can cause severe acute disease leading to morbidity and death in healthy individuals of all age groups and persistently remains one of the leading causes of virus-related death in the world <sup>[22]</sup>. Notably, influenza virus was responsible for the most lethal epidemic in human history since the bacterial plagues of the Middle Ages. From 1918 to 1920, an influenza outbreak, coined the “Spanish flu” at the time, resulted in the death of over 20 million people <sup>[2]</sup>, and influenza virus continues to remain a deadly presence in human life. Every year, IAV causes around 3,000,000 cases of severe respiratory disease and is responsible for the death of approximately 290,000 - 650,000 people <sup>[31]</sup>. Due to IAV’s propensity for zoonotic infections, influenza epidemics also result in significant economic losses every year due to morbidity and mortality in animals <sup>[21]</sup>. This wide range of host species also increases the potentiation for genomic reassortment between human-infecting influenza viruses and the influenza viruses of other host species, which exacerbates the pervasive threat of a pandemic outbreak by novel influenza viral strains <sup>[33]</sup>.

IAV is a single-stranded, negative-sense RNA virus belonging to the *Orthomyxoviridae* family that primarily targets airway epithelial cells <sup>[35]</sup>. Each viral particle (**Figure 1**) contains a 13 Kbp genome that is composed of eight segments of RNA coated with nucleoproteins (NP) and small amounts of nuclear export proteins (NEP), which when assembled are referred to as viral ribonucleoproteins (vRNPs) <sup>[50, 4, 54]</sup>. The segmented genome encodes for at least 14 proteins through the implementation of splicing and alternative open reading frames, which



allows at least three of the vRNPs to produce more than one protein [50]. The vRNPs are additionally bound to a viral polymerase complex formed of three proteins: polymerase basic 1 (PB1), polymerase basic 2 (PB2), and polymerase acid (PA). The eight vRNP-polymerase complexes are encased in an icosahedral capsid formed of the matrix protein, M1, which also contains a bound, non-structural protein, NS1. This capsid is further enveloped by a host-derived lipid membrane that contains several surface proteins including hemagglutinin (HA), neuraminidase (NA), and matrix-2 (M2) ion channel proteins [30, 55, 50].



**Figure 1: Diagram of an influenza A virus particle.** From outer layer to inner layer: the hemagglutinin (HA), neuraminidase (NA), and matrix-2 (M2) proteins are bound to the lipid

membrane. The capsid formed by the M1 protein layer lies underneath this membrane. Nuclear export protein/non-structural protein 2 (NEP/NS2) is bound to the M1 layer. Eight vRNA segments are coated with nucleoprotein (NP) and are bound to polymerase complexes formed of three proteins (PB1, PB2, and PA). Created with BioRender.com

As an obligate intracellular parasite, IAV is dependent on hijacking host cell machinery to promote replication, which can be divided into five distinct stages: entry of the virion into the host cell, importation of the viral genome (vRNPs) into the host nucleus, genome transcription and replication, export of vRNPs from the nucleus, and virion assembly and budding at the host plasma membrane <sup>[50]</sup>. The various proteins encoded by the IAV genome serve to facilitate this process (**Table 1**).

**Table 1: IAV RNA segments, proteins, and functions**

vRNP Segment	Protein	Function
1	PB2	Component of RNA polymerase Exonuclease activity for 5' cap "snatch"
2	PB1	Component of RNA polymerase Translation elongation
3	PA	Component of RNA polymerase Endonuclease activity
4	HA	Attachment to sialic acids on host cell surface
5	NP	vRNP nuclear import and export
6	NA	Sialic acid cleavage for release
7	M1 M2	Matrix protein Ion channel
8	NS1 NS2/NEP	Innate immune system antagonist vRNP nuclear export

Hemagglutinin (HA), a homotrimeric glycoprotein embedded in the viral lipid envelope, is responsible for initiating infection and binds to membrane receptors containing sialic acid on

the host cell, which facilitates virion entry into epithelial, macrophage, and dendritic cells via receptor-mediated endocytosis [55, 50, 47]. Due to the relatively low pH inside the endosome, conformational changes occur in HA that trigger the HA-facilitated fusion of the viral lipid membrane and the endosomal membrane. The low endosomal pH also causes a conformational change in the M2 protein, a transmembrane ion channel that is selective for protons. The influx of protons acidifies the viral core and promotes the release of the vRNPs from within the M1 protein capsid. With the fusion of viral and host membrane complete, the vRNPs are released from the endosome through the fusion pore into the host cell cytoplasm [27, 50].

Transcription and replication of IAV's genome occurs in the host nucleus, so the vRNPs must be transported to the nucleus by its associated proteins (NP, NEP, PA, PB1, and PB2). All vRNP-associated proteins are known to have nuclear localization signals, which are amino acid sequences that mark a protein for nuclear import. These tags allow the vRNPs to bind to cellular machinery that facilitates the entry of the viral genome into the host cell nucleus [50, 7].

Once inside the nucleus, the RNA components of the vRNPs are used as templates for both replication and transcription. Because the RNA of IAV's genome is single stranded and negative-sense, replication of the viral genome requires the creation of a positive-sense intermediate called complementary RNA (cRNA), which is subsequently used as a template to replicate new negative-sense viral RNA (vRNA). Replication of the vRNA can commence via the viral polymerase complex (PB1, PB2, and PA) without the presence of a primer due to complementary elements at the 5' and 3' ends of the genome, which allows the vRNAs to form various double stranded conformations that enable polymerase activity [4].

The viral polymerase complex is also required for the transcription of vRNA into mRNA. To produce mRNA ready for translation, the virus hijacks elements of the host cell machinery to transcribe mRNA for the 14 genes encoded in the genome <sup>[4]</sup>. Although the vRNP-associated proteins are not capable of producing a 5' methyl cap, PB2 has endonuclease activity that allows the protein to “snatch” methylated cap fragments (10 - 15 bps) from cellular mRNAs, which are then used by the viral RNA polymerase to initiate transcription <sup>[46]</sup>. In order to produce all 14 proteins from 8 segments of vRNA, host splicing machinery is also hijacked to express multiple proteins from vRNA segments 7 and 8. To do so, viral protein NS1 binds to small nuclear RNAs (snRNA) and other host splicing machinery and causes them to localize to and act upon the viral mRNAs. A secondary effect of this machinery hijacking is the decreased level of splicing of cellular mRNA, thereby inhibiting the host's ability to successfully express its own genome. NS1 further inhibits normal cellular genomic expression by preventing the export of cellular mRNAs by binding to the cleavage and polyadenylation specificity factor (CPSF), which prevents the maturation of cellular pre-mRNAs. However, the viral mRNAs are not thought to be matured by these hijacked CPSFs. Rather, the viral mRNAs are adenylated through a stuttering process caused by the presence of poly-U sequences in the viral genome. Once the poly-A tails are synthesized, the mature viral mRNAs are subsequently exported from the nucleus for translation into the various viral proteins <sup>[50, 34, 7]</sup>. vRNP-associated proteins, including nucleoprotein (NP) and the three subunits of the viral polymerase (PB1, PB2, and PA), are imported back into the nucleus after synthesis for vRNP assembly. Additionally, newly formed NS1 and NEP proteins are also imported into the nucleus and regulate several nuclear processes including nuclear export <sup>[7]</sup>.

After the replication of new vRNA, synthesis of new proteins, and formation of new vRNPs is complete, the nascent viral particles exit the nucleus via interaction with the CRM1-dependent pathway, a host mechanism commandeered by IAV to export vRNPs through the host's nuclear pores into the cytoplasm. NP and NEP, which are bound to the vRNA, are both known to bind with CRM1 to facilitate this export. It has also been demonstrated that NEP directly binds with the viral M1 protein, and M1 in turn binds to the negative sense vRNPs. This complex of vRNA, viral proteins, and CRM1 allows for the nuclear export of vRNPs [7].

Once the vRNPs have successfully entered the host cytoplasm, the viral material begins to localize at lipid raft domains at the apical plasma membrane of the infected cell. By this point, all viral proteins, including HA, NA, and M2 have been transported by the trans-golgi network through the cytoplasm and are localized at the apical plasma membrane [4]. New virus particles bud from the host plasma membrane, which provides the new virions with a lipid envelope that the proteins HA, NA, and M2 embed within. These new, membrane-enveloped virions anchor at the surface of the cell through binding interactions between HA and sialic acid-containing receptors [47, 50]. In order for the virus particles to release from the host membrane, neuraminidase (NA) must enzymatically break the bonds between HA and sialic acid residues. This cleavage of sialic acid not only allows the virion to be released from the host cell but also prevents virions from binding together by removing any sialic acid present on the carbohydrates present on HA itself. The release of virion particles completes the replication cycle of influenza [4]. The virus particles then go on to infect neighboring cells while the originally infected cell typically perishes due to various causes including the cytotoxic effects of the viral infection as well as programmed cell death directed by the immune response [11].

Understanding the details of the influenza replication cycle provides valuable insight into how, as well as when, cellular mechanisms attempt to block viral replication and provides clues as to what genes are instrumental in halting the infection. As humans and IAV co-evolved over the evolutionary timeline, the tug-of-war between pathogen and host has produced numerous mechanisms and counter-mechanisms that research has continued to illuminate. In order to discern the specific mechanisms that allow cells to clear viral infections, a general understanding of the host's varied responses to infection is essential.

### ***Cellular immune response to IAV infection typically results in cell death***

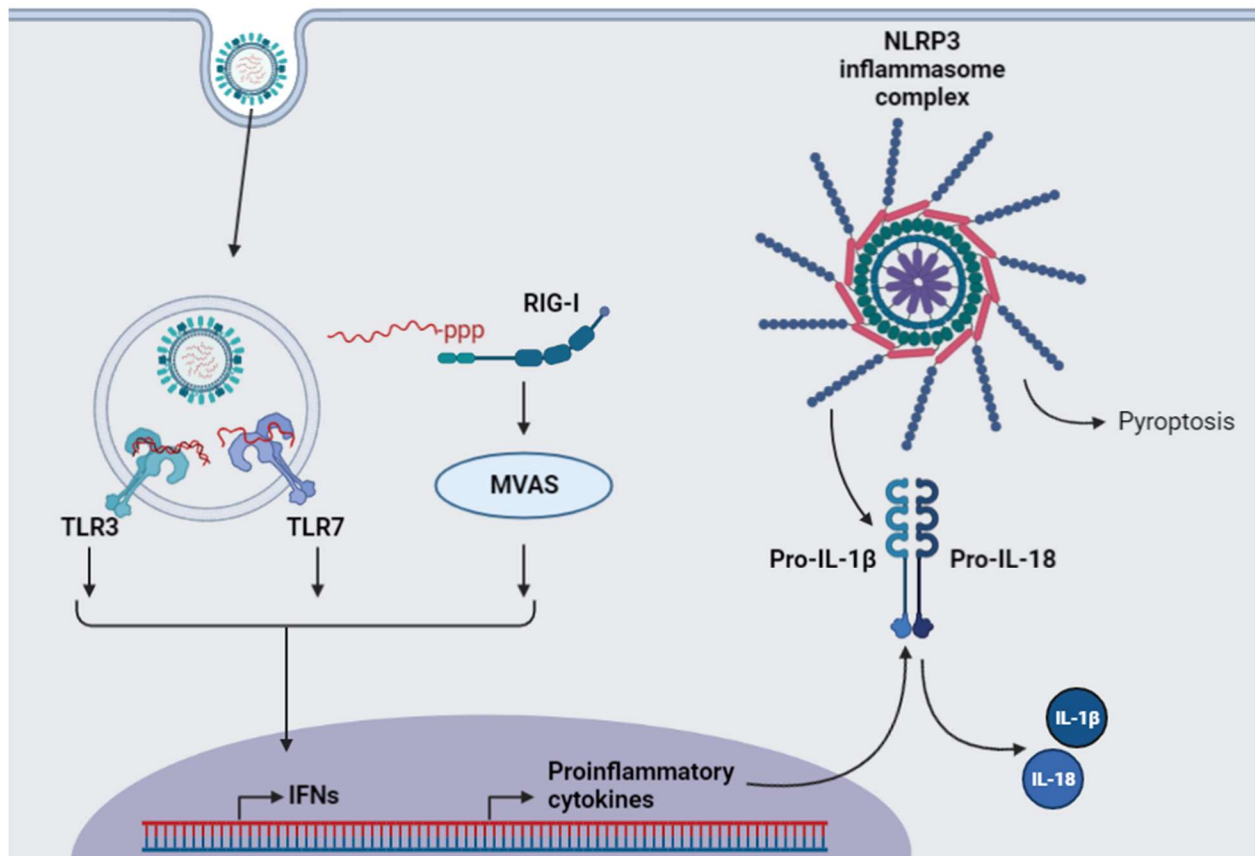
Influenza's entry into the host cell and the initiation of infection leads to the induction of the innate immune response within the cell. This response is triggered by the recognition of conserved molecular viral motifs called pathogen associated molecular patterns (PAMPs) by cellular pattern recognition receptors (PRRs), which are capable of sensing a wide range of PAMPs. In the case of viral infections, these motifs are typically RNA features that are not commonly present in cellular RNAs such as double-stranded RNA or the presence of 5'triphosphate (5'ppp) or 5'-diphosphate (5'pp) moieties. PRRs are instrumental to distinguish foreign material in the host cell, and in the case of IAV, both single-stranded and double-stranded vRNAs can be recognized by specialized PRRs such as Toll-like receptors (TLRs), RIG-I-like receptors (RLRs), and nucleotide-binding oligomerization domain, leucine-rich, repeat-containing receptors (NOD-like receptors (NLRs)). These receptors each play specific roles in detection of influenza. TLR3 and TLR7 are both implicated in recognizing extracellular vRNA as well as vRNA in endosomal compartments during the early stages of infection; however, TLR3 detects dsRNAs while TLR7 detects ssRNAs [11]. Once the viral RNAs have

been released into the host cytoplasm, the viral material can be detected by cytosolic RIG-I receptors, which most efficiently recognizes the 5'ppp and 5'pp dsRNA moieties. Activation of these and other PRRs leads to the induction of subsequent antiviral mechanisms [21, 33, 51].

The detection of PAMPs by PRRs in the TLR and RLR families (**Figure 2**) ultimately results in the induction of cytokines and chemokines, such as type I interferons (IFNs), including interferon- $\alpha$  (IFN- $\alpha$ ) and interferon- $\beta$  (IFN- $\beta$ ) [14]. Interferons are key, non-specific antiviral proteins secreted by infected cells that act as signaling molecules in the cellular defense against viral infections, and the binding of these interferons to their cognate receptors, interferon- $\alpha,\beta$  receptors (IFNARs), initiates a signaling cascade via the Janus kinase-signal transducer and activator of transcription (JAK-STAT) pathway [32, 54]. This critical pathway activates hundreds of different interferon stimulated genes (ISGs) that create an 'antiviral state' that aims to inhibit the replication of the invading pathogen through direct and indirect mechanisms [14, 42]. The activated ISGs generate this antiviral response in a variety of ways that can impact all stages of viral replication, including binding and neutralizing viral genomes in the cytoplasm, targeting and cleaving viral RNA, inhibiting protein transportation in the endoplasmic reticulum and nucleus, restricting viral RNA replication, inhibiting viral protein translation, modifying cellular membrane proteins, regulating other cellular ISGs, and commonly, inducing programmed cell death via apoptosis [14, 32, 21].

Similarly, the detection of PAMPs by NLRs also frequently results in programmed cell death. The presence of viral PAMPs activates receptors of the NLR family, the most widely studied of which is NLRP3. Activation of NLRP3 during infection leads to the assembly of large multimeric complexes called inflammasomes. Once assembled, inflammasomes mediate the

activation of caspase-1, which subsequently leads to the processing and release of proinflammatory cytokines, such as pro-IL-18, within the infected cells. This leads to another form of cell death, pyroptosis, during which the cell membrane ruptures and messenger cytokines are released into the extracellular matrix to influence neighboring cells [35].



**Figure 2: Detection of IAV by PRRs triggers the innate immune response.** IAV enters the host cell via endocytosis. After the viral contents are released from the endosome, viral genomic



ssRNA and dsRNA is detected by endosomal receptors TLR7 and TLR3, respectively. Once the vRNA enters the cytoplasm, cytosolic RIG-I sensors detect 5'-diphosphates and 5'-triphosphates present on vRNA, which initiates the MAVS-IRF3-type I IFN signaling cascade. Detection of IAV by these sensors leads to induction of IFNs and proinflammatory cytokines. Accumulation of these proinflammatory cytokines activates NLR receptors, which initiates assembly of the NLRP3 inflammasome complex. This complex mediates the release of interleukins and induces an inflammatory form of cell death, pyroptosis. Created with BioRender.com.

Overall, the expression of IFNs and the induction of ISGs play a key role in the outcome of a viral infection. Successful expression typically restricts the ability of a virus to replicate and can clear infection from the host with minimal immunopathology <sup>[14]</sup>. However, during an IAV infection, inhibition of IFNs and the associated ISGs by viral proteins, as well as cellular genomic degeneration caused by viral-induced oxidative stress, typically leads to cell death. Cell death, the predominant fate of IAV-infected cells, can be triggered through a variety of phenomena including pyroptosis, virus-directed apoptosis, and host-directed apoptosis, which results from either extrinsic or intrinsic pathways <sup>[10, 14, 33]</sup>.

Apoptosis, a ubiquitous, highly-regulated function of multicellular organisms to remove aging or damaged cells, is induced through the extrinsic pathway when cells of the immune system, notably cytotoxic T lymphocytes, detect virally infected cells through ligand-receptor interactions and the presence of viral-induced chemokines <sup>[9]</sup>. This form of extrinsic apoptosis is mediated by cytokine ligands of the tumor necrosis factor (TNF) superfamily, such as TNF-related apoptosis-inducing ligand (TRAIL) or FasL, that are produced by T cells when bound to cognate receptors on infected cells. These effector molecules induce a cascade of intracellular

pathways that results in cell death, presumably serving as a protective response to the rest of the organism by eliminating the cellular machinery needed for viral replication [14, 9, 44]. Whether apoptosis also promotes IAV dissemination remains unclear; however, it is known that IAV is capable of positively and negatively modulating extrinsic apoptosis through inhibiting antiviral signaling and affecting B cell antibody production [4].

Similarly, IAV detection by cellular PRRs can induce apoptosis via the intrinsic, or mitochondrial, pathway through the production and signaling of type I IFNs. The release of IFNs triggers apoptosis in most respiratory cells directly through caspase activation downstream of IFNAR. However, IAV can inhibit apoptosis during early stages of infection by upregulating the anti-apoptosis cellular pathway, phosphoinositide-3-kinase-protein kinase B (PI3K-Akt). This apoptosis repression is controlled by NS1, the viral protein known to play the largest role in viral-regulated apoptosis during infection, although viral protein PB1-F2 has also been implicated in playing a pro-apoptosis role. NS1 is also known to further inhibit apoptosis through the attenuation of type I IFN production, interactions with heat shock protein 90 (HSP90) and alpha tubulin, as well as inhibiting p53-mediated transcriptional activity [27, 4].

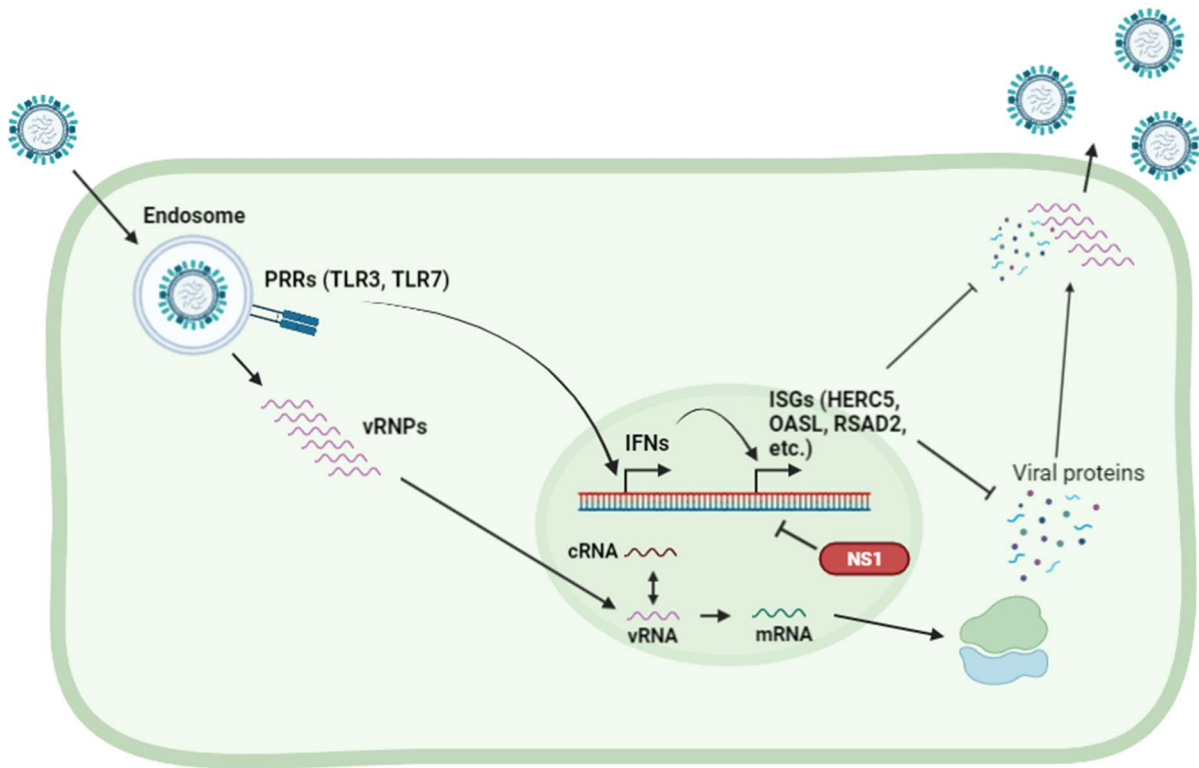
Alternatively, IAV is capable of promoting apoptosis through the suppression of the PI3K-Akt pathway as well as the upregulation of the pro-apoptosis pathway via p53. IAV-induced apoptosis is also facilitated by NP through the attenuation of the ring finger 43 (RNF43) protein [18]. RNF43 normally inhibits apoptosis by destabilizing p53, so by decreasing RNF43's impact on cellular activity, IAV can promote the induction of apoptosis. Viral protein M1 further promotes apoptosis through silencing of anti-apoptosis effect of heat shock protein 70 (HSP70). Overall, it has been implicated that NS1 plays a role in both the viral-induced activation and

suppression of apoptosis. By inhibiting apoptosis early on, IAV provides itself time for replication, and by promoting apoptosis after successful replication, the virus particles are more easily released from the host cell to infect neighboring cells [4].

While early host-induced apoptosis can reduce the overall pathological severity of an IAV infection, hosts have evolved additional mechanisms encoded in antiviral genes that attempt to clear an active infection from the cell. However, IAV has co-evolved strategies and proteins that can inhibit the host's infection response [10, 33]. In order to circumvent these cellular antiviral mechanisms, viral proteins such as NS1 play an integral role in the virus's ability to negate host defenses and enhance the probability of successful viral replication [31]. One of the first cellular responses a virus must overcome is IFN signaling. NS1 targets and inhibits the activation of multiple components of IFN induction, including interferon regulatory factor 3 (IRF3), which limits IFN production, signaling, and subsequent ISG expression [27]. NS1's suppression of IFN production also inhibits early, IFN-induced apoptosis thereby providing sufficient time for IAV to successfully replicate [14, 33, 4]. To further enable replication and overcome host defense, IAV's NS1 performs a variety of other functions through interactions with cellular mechanisms. This 26kDa viral protein has three distinct domains including an N-terminal RNA-binding domain, an effector domain located in the middle of the protein, and a C-terminus tail. Each domain is capable of interacting with distinct cellular factors. In addition to suppressing IFN production, interfering with IFN signaling pathways, and regulating apoptosis, NS1 also limits cellular mRNA transcription [27].

Through several proposed mechanisms, NS1 is able to inhibit host mRNA translations, including the expression of ISGs (**Figure 3**). First, NS1 interacts with host proteins associated

with gene transcription including cleavage and polyadenylation specificity factors (CPSF30) and poly(A)-binding protein II (PABII). In routine function, CPSF cleaves consensus sequences of cellular pre-mRNA, and PABII facilitates polyadenylation of the 3' end of pre-mRNA. Binding of these cellular proteins to the effector domain site of NS1 inhibits normal 3' processing of pre-mRNA. The disrupted pre-mRNA can then be cleaved by the viral protein PB1 and processed into a primer for viral mRNA transcription by PB1, which also acts as an RNA polymerase for viral replication. This action both directly enhances IAV replication as well as leads to the accumulation of unprocessed mRNA in the nucleus and the significant reduction of mRNA translation. Additionally, NS1 is capable of blocking the nuclear export of matured cellular mRNA through interactions with multiple protein complexes that form the nuclear export machinery in the host. Lastly, certain IAV strains possess NS1 proteins that contain histone-like sequences at the C-terminus that bind to transcription factors such as human PAF1 transcription elongation complex (hPAF1C). By binding to hPAF1C, NS1 inhibits elongation during the transcription of the host genome, including antiviral genes [27, 2]. Although it was previously known that NS1 binds to dsRNA to prevent cellular detection of the IAV transcriptome, it has recently been discovered that NS1 can also bind in a similar manner to cellular dsDNA to diminish the expression of ISGs [5]. These mechanisms allow NS1 to significantly reduce host antiviral defenses through the suppression of transcription as well as the prevention of cellular pre-mRNA maturation and nuclear export.



**Figure 3: NS1 inhibits expression of interferon stimulated genes (ISGs).** IAV enters the cell via endocytosis, which later fuses with the viral envelope, releasing the viral genome for import into the host nucleus. The detection of viral components by PRRs triggers the production of IFNs, which in turn induces ISG expression. This expression is inhibited by NS1 through several mechanisms and allows for the transcription and replication of the viral genome as well as the synthesis of new viral proteins. Created with BioRender.com.

Since IAV relies on host ribosomes to translate viral mRNA, reducing the amount of cytosolic cellular mRNA also increases the rate of viral protein synthesis. NS1 is further capable of enhancing translation of viral mRNA by blocking host dsRNA sensors that would normally

prevent viral translation. Under unencumbered cellular conditions, protein kinase R (PKR) identifies dsRNA and directly phosphorylates the alpha subunit of the eIF2 translation initiation factor (eIF2 $\alpha$ ). The phosphorylation of eIF2 $\alpha$  globally inhibits the initiation of translation in the cell; however, NS1 binds directly to PKR and prevents the phosphorylation of eIF2 $\alpha$ , which is believed to block the inhibitory activities of PKR. By preventing the host from blocking global translation, viral mRNA is able to associate with cellular ribosomes and initiate translation [27].

Furthermore, NS1 is capable of suppressing host immunity by preventing detection by cellular proteins. Since recognition of IAV triggers the innate immune response, NS1 has evolved to reduce the ability of the cell to detect the virus. Because transcription and replication of IAV's negative-stranded RNA requires the creation of positive-stranded cRNA, dsRNA can form during this process. During viral infection, PKR blocks both cellular and viral protein synthesis when dsRNA is detected, thereby inhibiting viral replication. However, the N-terminal of NS1 can bind to dsRNA, which blocks the activation of PKR [53]. This protein-vRNA binding activity thereby reduces the cell's ability to detect vRNA and prevents the translation of viral proteins [2]. Additionally, NS1 is capable of sequestering dsRNA, which limits the detection of dsRNA by the cellular sensor RIG-I, a virus recognition protein vital for initiating the MAVS-IRF3-type I IFN signaling cascade that induces the production of type I IFNs [26, 33, 25]. RIG-I can also be directly inhibited via NS1 targeting of TRIM25, a ubiquitin ligase that acts as a regulator molecule in the innate immune system. Under uninhibited circumstances, TRIM25 mediates the ubiquitination of RIG-I receptors, which leads to production of IFNs; however, a domain within NS1 is capable of interacting with a coiled domain of TRIM25 to inhibit the ubiquitination of RIG-I [19]. IAV mutants lacking this NS1 domain have demonstrated reduced virulence due to the inability to inhibit RIG-I detection [48]. The N-terminal dsRNA binding domain of NS1 also

prevents detection of viral dsRNA by the ISG protein, 2'-5' oligo (A) synthetase (OAS), which when activated, induces the activity of RNase L, a key enzyme involved in the cleavage of viral RNAs. Therefore, it is likely that a key role of NS1 is to bind to viral dsRNA to prevent both RNA detection by PRRs as well as RNA destruction by the OAS/RNase L pathway [41].

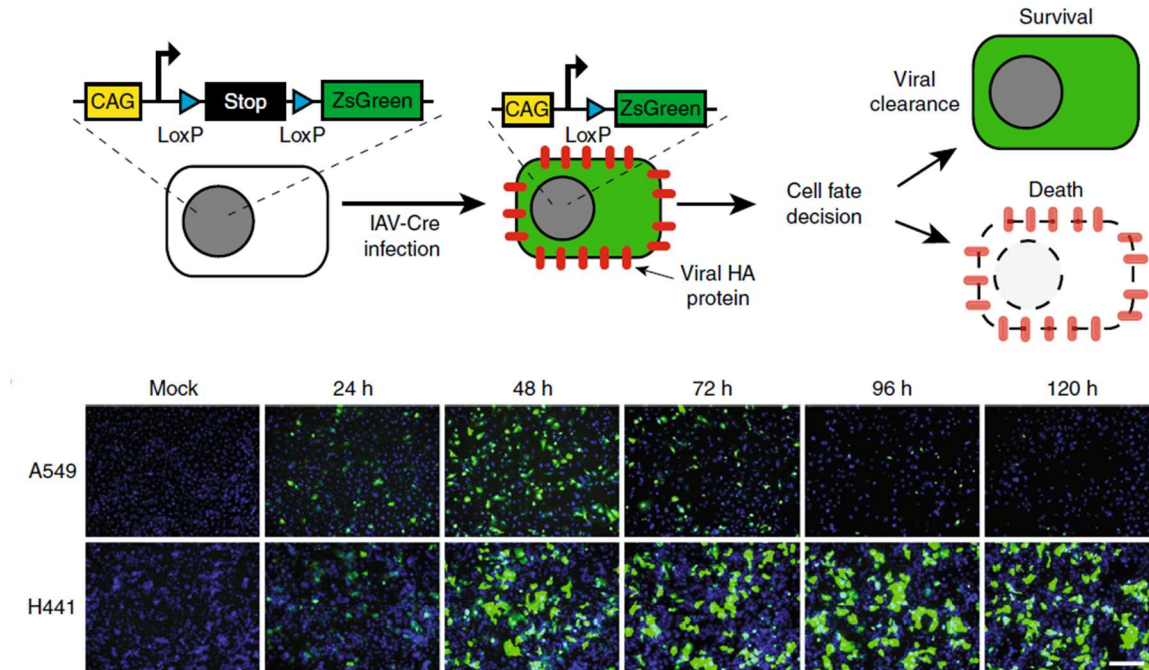
Viral hosts have evolved numerous measures to stop the replication of IAV and minimize the pathological impact of infection. In general, the host attempts to minimize the deleterious effects of influenza infection by sacrificing infected cells through pyroptosis or apoptosis, whether they be triggered by the infected cell itself or by immune cells. IAV, in general, attempts to delay cell death in order to successfully replicate, and, over the course of an evolutionary timeline, is capable of negating host cell death programs and continues to be an effective pathogen. Viral proteins, particularly NS1, are highly capable of ensuring successful replication through a variety of mechanisms including delaying apoptosis, inhibiting cellular transcription and translation, and preventing cellular recognition of vRNA. Because IAV is exceedingly adept at negating host defenses, the ultimate fate of nearly all infected respiratory cells is death whether directly caused by the virus-induced cell lysis or induced by the host to mitigate further damage. However, recent research has determined that there are exceptions to this rule, and certain cells within the respiratory system are capable of winning the battle between host cell and IAV.

### *Club cells can survive direct infection with influenza A virus*

The long-term fate of IAV-infected cells is impacted by a number of events, including recognition and clearance by the adaptive immune system, innate cellular antiviral pathways triggering apoptosis, and viral necrosis. As such, it was previously believed that death was the ultimate fate of all cells that IAV directly infects. However, a subset of respiratory epithelial cells, called club cells, have demonstrated the ability to survive and persist when infected with IAV. Club cells are non-ciliated cells found on the luminal surface of airways that, although poorly studied, are believed to secrete surfactants within the respiratory system and may play a role in repairing injured airways [6, 13]. Club cells are one of many cell types, along with ciliated, goblet, and basal cells, that form the epithelium in human respiratory systems and are notably the only cell type that are known to be capable of non-lytically clearing IAV infections [10, 28, 41].

Multiple studies have investigated what makes club cells unique during influenza infection in an effort to better understand their survival mechanisms. More recently, a study of two respiratory cell types, human lung adenocarcinoma club cell lines (H441) and alveolar epithelial cell lines (A549), during IAV-infection has demonstrated a significant difference in mortality rate. Notably, only H441 cells were capable of surviving IAV infection stemming from the cell's ability to successfully clear the virus (**Figure 4**). The ability of club cells to clear and survive infection is directly due to their expression of an effective antiviral response. Although it is likely that all epithelial cells contain the genomic information to potentially produce this response, the interference from viral proteins along with the genomic instability caused by virus induced-reactive oxygen species (ROS) prevents sufficient expression in non-club cells [10, 49].





**Figure 4: H441 cells survive IAV infection.**<sup>[10]</sup> The ZsGreen-Cre-reporter system (above) irreversibly labels cells that have been infected by Cre-expressing IAV with green fluorescence. A549 and H441 cells were both infected with IAV. The A549 cells become infected, express the ZsGreen reporter, but then succumb to cell death. Alternatively, a large proportion of H441 cells survive infection and continue to express the ZsGreen reporter (below).

Influenza virus infections are characterized by inflammation and an increase in oxidative stress caused by excessive generation of reactive oxygen species, such as superoxide anion ( $O_2^{\cdot-}$ ), hydroxyl radical ( $\cdot OH$ ), and non-radical hydrogen peroxide ( $H_2O_2$ ), produced by host responses<sup>[39, 45, 8]</sup>. It has furthermore been suggested that IAV is directly responsible for inducing ROS production in lung epithelial cells under experimental conditions. Examination of 8-hydroxy-2'-deoxyguanosine (8-OHdG) levels, a common biomarker of ROS-induced DNA damage, in IAV-infected respiratory cells demonstrated IAV's direct role in the increase of ROS-

mediated damage <sup>[10]</sup>. Under typical circumstances, ROS are produced by the cell as byproducts of normal mitochondrial metabolism and other enzymatic processes, and cells are typically able to mitigate these oxidants via antioxidants and enzymes, such as superoxide dismutases (SOD) and superoxide reductases, to maintain a functional homeostasis. However, during IAV infection, the production and accumulation of ROS surpasses the cell's ability to remove or convert these molecules <sup>[39, 8]</sup>.

Under these infectious conditions, the abundance of ROS disrupts the intracellular redox balance and leads to high levels of oxidative stress causing systemic cellular instability and toxicity as ROS begins to interact with and irreversibly destroy a variety of cellular molecules including proteins, lipids, carbohydrates, and nucleic acids <sup>[38]</sup>. In particular,  $\cdot\text{OH}$  causes the greatest impact on host DNA as it is reactive with both purine and pyrimidine bases as well as the sugar moiety of the DNA backbone <sup>[8]</sup>. If this DNA damage accumulates without correction, the damage can inhibit the cell's ability to express and produce an effective antiviral response. This reduction of gene expression along with other cytotoxic effects of viral infection blocks the cell from clearing the virus and results in cell death in non-club cells.

Although the effects of ROS can be adverse, at lower levels, the reactive species do play a beneficial role in the cellular immune response. When ROS levels are slightly above baseline, they have been shown to promote production of antiviral cytokines such as interferons, tumor necrosis factors, interleukins, and chemokines, which signify that ROS can act as a promoter of the antiviral inflammatory response. Furthermore, it has been shown that certain PRRs, such as TLRs, RLRs, and NLRs, are activated by the presence of ROS, which can trigger beneficial host-directed death through various pathways <sup>[39, 35]</sup>. However, at higher levels, ROS generates a

pathological level of inflammation and is adverse to cell survival, particularly due to the disruption that oxidative DNA damage causes to reduce gene expression <sup>[39]</sup>.

At these higher, pathological levels, oxidative stress damages the host cell's DNA, including lesions that lead to unstable genomic mutations and cell death. Research observing DNA repair loci has demonstrated that significant increases of double-stranded breaks (DSBs) occur in the DNA of cells infected by IAV. During this period of excessive ROS production, DNA repair mechanisms are essential to mitigating genetic damage and preventing cell death as well as modulating the overall infection outcome <sup>[37]</sup>. Specifically, it has been experimentally demonstrated that the DNA mismatch repair (MMR) pathway, a widely-conserved system responsible for detecting and repairing single nucleotide errors that spontaneously arise during DNA replication as well as during oxidative DNA damage caused by ROS <sup>[29, 8]</sup>, plays a key role in the repair of ROS-damaged DNA. In a comet assay, a gel electrophoresis-based method used to measure DNA breaks in eukaryotic cells by first producing nucleoids containing supercoiled loops of DNA from lysed cells. Then, electrophoresis of these nucleoids is performed in a high pH environment. The results, observed under fluorescence microscopy, resemble comet tails whose length is dictated by the number of breaks in the DNA - presumably due to the loss of supercoiling at breaks in the DNA, which is then free to travel towards the anode <sup>[43, 13]</sup>. During the study, IAV-infected H441 cells were treated with the restriction enzyme Fpg, which cleaves DNA at sites of oxidative damage thereby allowing for the quantification of oxidative damage via comet assay. Fpg-treated cells either had normal, functional MMR pathways or siRNA-suppressed MMR expression. Cells without functional MMR produced significantly longer comet tail lengths, indicating that without MMR, oxidative damage to DNA from IAV infection is significantly greater <sup>[10]</sup>. Maintaining MMR function is

critical to preventing widespread genomic damage during IAV infections, and therefore is likely also key for club cells to maintain the ability to express the necessary antiviral genes to clear the virus.

The impact of ROS on an infected cell's ability to express antiviral genes is compounded by the ability of IAV to suppress the action of the MMR mechanism. Although it has been demonstrated that DNA repair pathways are downregulated during IAV infections in the majority of cell types, previous research has determined that, unlike other respiratory cells, club cells uniquely preserve the function of MMR during infection, thereby reducing the deleterious impact of viral induced-ROS and allowing the cells to sufficiently express antiviral genes. During the study of H441 and A549 cells, an siRNA loss-of-function screen was conducted to identify genes that contribute to club cell survival when challenged with IAV. Among the validated genes was *MSH6*, a gene encoding a key protein of MMR. To further evaluate MMR's impact on H441 cell survival during IAV infection, other key proteins of MMR (MSH2, MLH1, PMS2, and EXO1) were also knocked down individually, all of which resulted in reduced survival regardless of which protein was suppressed. Furthermore, MMR protein levels were compared between A549 cell and H441 lines, and while A549 cells lost >25% of their MMR activity, the MMR activity of infected H441 cells was consistent with activity levels in control, mock-infected cells. These results indicate that IAV survival in club cells is directly related to the cell's ability to mitigate genetic damage caused by the accumulation of virus-induced ROS through a preserved MMR pathway <sup>[10]</sup>.

Previously, the link between MMR activity preservation and antiviral gene expression had not been determined; however, recent research has presented evidence that a reduction in

MMR activity reduces the host cell's innate antiviral transcriptional response to IAV. By generating oxidative damage in H441 cells with hydrogen peroxide (H<sub>2</sub>O<sub>2</sub>) treatments, it has been demonstrated that both RNA expression and protein levels of ISGs are significantly reduced in cells exposed to high levels of ROS. By repeating this experiment with MMR proteins knocked down, it was observed that ISG expression is even further reduced, signifying MMR's role in maintaining ISG expression. Moreover, during an evaluation of 58 ISGs induced by IAV infection, it was determined that the expression of 28 of these genes was significantly reduced when the H441 cells were transfected with *MSH2* and *MSH6* siRNA to inhibit MMR activity. Overall, our current understanding suggests that ISG expression is significantly attenuated during IAV infection by virus-induced ROS and downregulation of DNA repair pathways; however, in the case of club cells, MMR is preserved and the expression of key antiviral genes is maintained, allowing for club cell survival of the virus [10].

The ability of club cells to survive and clear IAV infection has been demonstrated to, at least in part, be a result of DNA MMR pathway preservation. Resisting viral downregulation of MMR pathways allows the cells to repair ROS-induced DNA damage and fully express antiviral genes. While other cell types succumb to nearly certain death during IAV infection, this innate ability of club cells allows them to survive infection through a process termed non-lytic clearance.

### *Non-lytic clearance occurs in several viral infections but is poorly understood*

In the course of a typical IAV infection, a wide variety of cells within the respiratory tract are invaded and subsequently challenged by IAV's replication cycle. Typically, IAV infection in the host cell is resolved through either virus- or host-induced apoptosis or removed by cells of the adaptive immune system [28]. However, recent studies have demonstrated that some infected cells, namely club cells, are capable of clearing the infecting virus non-lytically, signifying that the cells degrade the infecting virus and continue to survive after viral clearance [10]. While this phenomenon is incompletely understood at present, the ability to clear viral infections in this manner has been observed outside of IAV and club cells.

Different cell types mount unique responses to viral infection based upon their unique basal gene expression profile, and as such, have a variety of responses to infection, some of which confer the ability to clear viruses. Apart from certain lung epithelial cell types that are known to clear either influenza A or influenza B viruses [10, 16, 17], there are other cell types that are known to be capable of non-lytically clearing other viruses. Similarly, hepatocytes are capable of non-lytically clearing lymphocytic choriomeningitis virus (LCMV) through an unknown mechanism [23]. Hematopoietic cells have likewise demonstrated the ability to non-lytically clear hepatitis B virus, although the exact mechanism is believed to be dependent on interactions with immune cells [24]. Furthermore, it is known that neural cells are able to clear viral infection and continue to survive in the long-term against several viruses including the rabies virus, Sindbis virus (SINV), and murine coronavirus (M-CoV) [22, 42, 20].

While the key antiviral genes required for non-lytic viral clearance have yet to be identified, the purpose of non-lytic viral clearance in hosts, rather than clearing infection through cell death, has been evaluated in several cell types. Although immune-directed apoptosis has long been understood to be an effective defense mechanism for multicellular organisms challenged with infection, non-lytic clearance and cell survival also plays a beneficial role during active and post-infection periods. During respiratory infections, the epithelium is subject to widespread cellular damage and death, which can weaken the epithelial barrier and lead to secondary infections of the respiratory system by other pathogens. The preservation of cells in this area is therefore advantageous to reducing overall pathology, so the survival of club cells during an active IAV infection has clear benefits <sup>[16]</sup>. Additionally, experimentation on club cell function has demonstrated that club cells are capable of inducing apoptosis in neighboring, damaged alveolar cells <sup>[3]</sup>. Although the exact function of club cells remains controversial, it is possible that this ability to induce apoptosis in other cells provides another benefit to the host during active IAV infections by further decreasing overall pathology stemming from club cell survival.

A similar protective role is observed in the infection of olfactory sensory neurons (OSNs) of the upper respiratory tract by influenza B virus (IBV). By non-lytically clearing IBV, these cells maintain the integrity of the local nervous system and likely protect the central nervous system from subsequent infection <sup>[18]</sup>. Non-lytic clearance is also observed in murine olfactory bulb interneurons when infected with rabies virus, which prevents the loss of these irreplaceable cells <sup>[57]</sup>. Furthermore, it has been demonstrated that LCMV, a virus capable of infecting a wide variety of tissues, can be cleared by cytokine-mediated, specifically IFN- $\gamma$  and TNF- $\alpha$ , mechanisms in parenchymal liver cells i.e. hepatocytes. However, the same virus is not known to

be non-lytically cleared from other cells it infects such as intrahepatic nonparenchymal cells or splenocytes. These latter cells do not possess the required factors to intracellularly neutralize LCMV that hepatocytes do, which are presumably present in hepatocytes due to the cell type's critical function in the liver [25]. If the selective pressure for non-lytic clearance in particular cell types is the preservation of vital host systems, club cells may have evolved this protective role in the respiratory epithelium, although the genetic basis is presently unclear.

While the non-lytic clearance of influenza virus from club cells has been directly observed and confers clear benefits to the host, the exact genetic mechanisms have not yet been explored. It has been previously demonstrated that epithelial cells that survive viral infection express distinct transcriptional profiles that significantly vary from uninfected cells, indicating that the antiviral state of infected cells capable of non-lytic clearance is correlated with the expression of specific antiviral genes [10, 16]. Several genes have been implicated in generating the complex antiviral state observed in club cells and are potentially responsible for club cell survival.



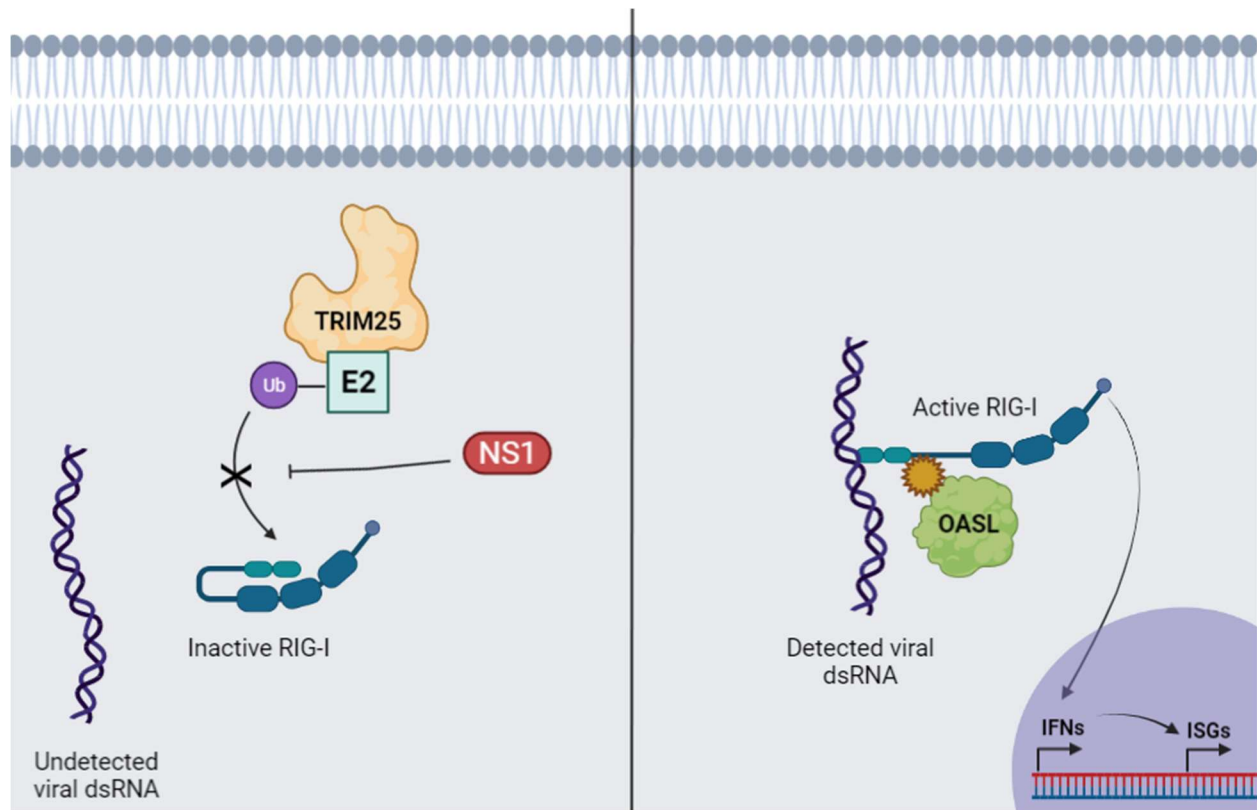
### *Key antiviral genes are critical for anti-influenza immunity*

Although the innate immune response against viruses is genetically complex and many genes are known to play roles in establishing an antiviral state in infection cells, it has not yet been determined which genes are critical for the non-lytic clearance of IAV from club cells. However, during an evaluation of protein fold change due to MMR knockdown during IAV infection in club cells, several ISGs and antiviral genes were downregulated, likely resulting in the inability of these cells to clear the virus <sup>[10]</sup>. These results suggest that during an infection of club cells, these genes remain active and are directly related to the ability of club cells to non-lytically clear influenza. Furthermore, previous observations of the antiviral function and mechanisms of several of these genes provides strong evidence of their link to clearance of IAV.

#### *OASL*

2'-5' oligoadenylate synthetase-like (OASL) protein, induced by IFN, plays a vital role in detecting and, potentially, degrading cytosolic vRNA in host cells. As a member of one of the most predominant ISG families, the OAS family, OASL is best-recognized for playing an antiviral role against a wide spectrum of RNA viruses <sup>[61]</sup>. Because IAV's RNA can form temporary double-stranded conformations, it is possible for PRRs, such as RIG-I, to detect its presence in the cytosol. In an effort to escape detection, NS1 is capable of inhibiting RIG-I activation in an effect to block the innate response; however, OASL is now known to be capable of activating RIG-I receptors that have been inhibited by viral NS1 (**Figure 6**). As previously discussed, RIG-I typically requires ubiquitination by TRIM25 to be active; however, NS1 is capable of inhibiting this process <sup>[19]</sup>. OASL is able to circumvent this viral mechanism by

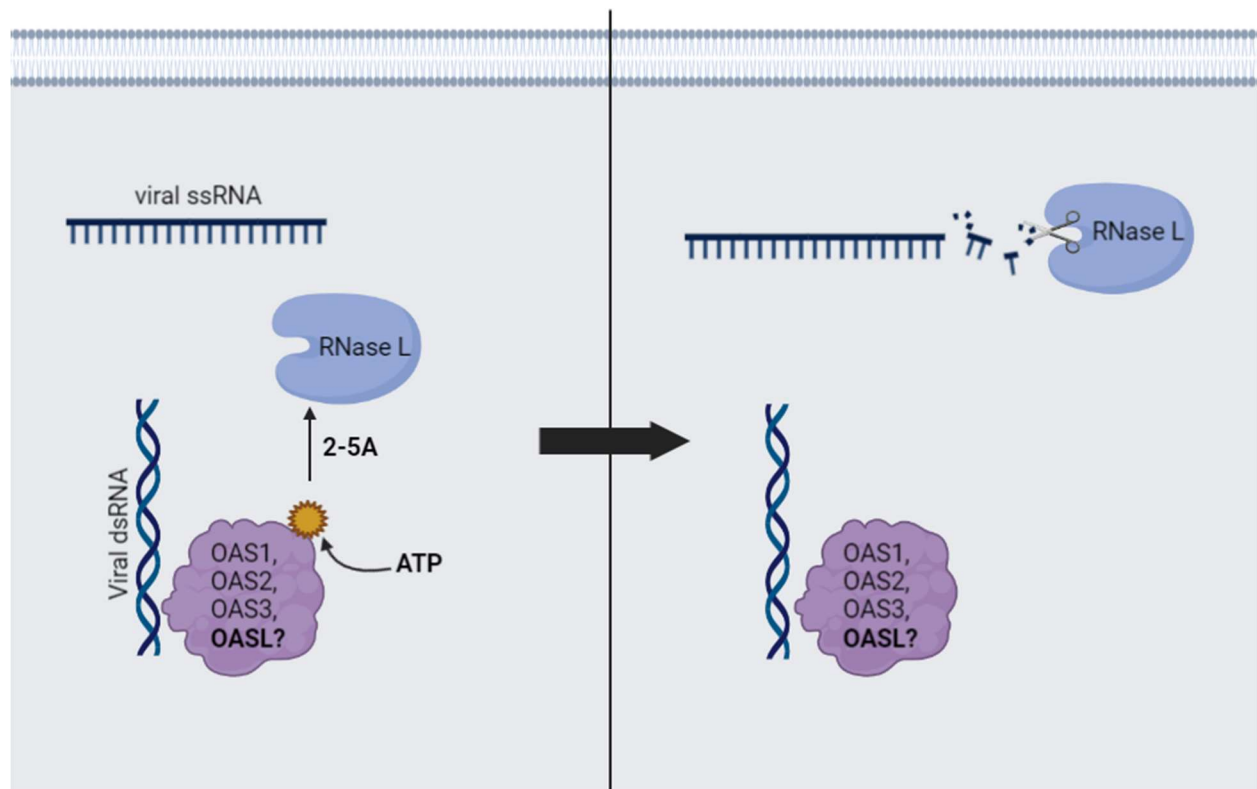
directly activating RIG-I by mimicking polyubiquitin, and due to this interaction, RIG-I-based viral detection is more sensitive and can detect IAV at lower virus levels when OASL is actively expressed. During a recent 2015 study, it was determined that loss of OASL function directly led to decreased RIG-I activity as well as a suppressed antiviral response downstream of RIG-I, which resulted in enhanced viral replication [61]. Furthermore, OASL-based RIG-I activation generally produces relatively lower IFN levels than normal RIG-I-induced IFN expression and reduces IFN toxicity, thereby also decreasing the overall severity of disease in the host [21]. Overall, OASL's ability to negate NS1's inhibition of RIG-I allows the PRR to induce an effective expression of IFNs, which subsequently leads to the upregulation of numerous ISGs involved in generating the antiviral state, including other members of the OAS family.



**Figure 5: OASL activates RIG-I through ubiquitin-like action.** In an attempt to avoid viral RNA detection, NS1 inhibits the TRIM25-mediated ubiquitination of RIG-I, thereby preventing the PRR's activation. To overcome this viral mechanism, OASL is able to activate RIG-I through a ubiquitin-like action. RIG-I is then able to detect the presence of viral dsRNA, which subsequently induces the production of IFNs and ISGs. Created with BioRender.com.

Detection of viral dsRNA by other OAS-family proteins, such as OAS1, OAS2, and OAS3, activates the OAS/RNase L signaling pathway, ultimately leading to the enzymatic activation of ribonuclease L (RNase L). When these OAS proteins encounter viral dsRNA, they bind to the viral genetic material and become enzymatically active. The active OAS proteins subsequently convert ATP into 2'-5'-oligoadenylate (2-5A), which goes on to trigger dimerization and activation of latent cellular RNase L [15]. Once activated, RNase L non-

selectively cleaves both cellular and viral mRNAs in the cytoplasm, which prevents viral protein translation from occurring, thereby halting IAV replication [56, 60, 21] (**Figure 7**). Furthermore, because the IAV genome is single-stranded, the non-selectivity of RNase L also allows it to destroy any viral genomic RNA presently located in the cytoplasm. The production of RNA fragments by RNase L additionally triggers increased activation of type I IFNs, thereby amplifying the antiviral response [15]. Because RNase L destroys all cytosolic ssRNA, including cellular mRNAs, the activation of RNase L is completely dependent upon and tightly regulated by the activation of its counterpart OAS proteins by cytoplasmic dsRNA present in infected cells, thereby reserving this potent and destructive function until viral infection is detected [15, 41]. It is currently thought that, unlike other OAS proteins, OASL is not enzymatically active and does not convert ATP to 2-5A, and therefore, only plays an RNase L-independent role during viral infection; however, it is possible that OASL's role has not yet been fully studied and appreciated. OASL's role in RIG-I activation has only recently been discovered, and it is possible that as a member of the OAS family, OASL too plays a more direct role in viral RNA degradation through the OAS/RNase L pathway. At a minimum, OASL indirectly contributes to the RNase L degradation of vRNA by increasing IFN levels in infected cells through RIG-I activation.



**Figure 6: OAS/RNase L pathway leads to viral dsRNA degradation.** Detection of viral dsRNA by latent OAS proteins activates them and triggers the conversion of ATP to 2'-5'-oligoadenylate (2-5A), which subsequently activates latent cytosolic RNase L. The activated enzymatic activity non-selectively degrades cytosolic cellular and viral ssRNA, thereby blocking viral protein translation. Although OASL is currently not believed to be catalytically active, future research may reveal an additional role in RNase L activation. Created with BioRender.com.

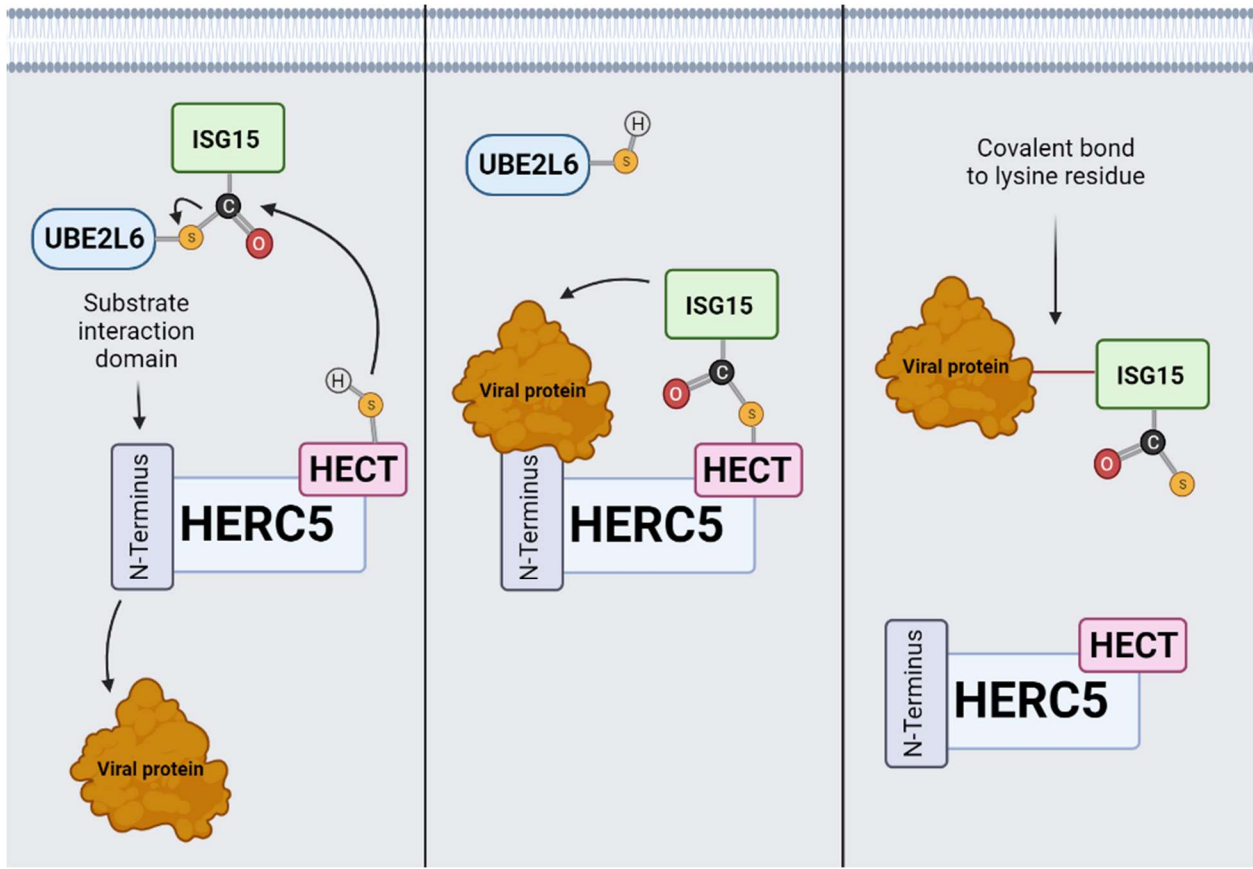
The role of OASL in RIG-I activation as well as its indirect role in the upregulation of other OAS proteins involved in vRNA degradation are known to occur in club cells. Transcriptome analysis of surviving club cells shows upregulation of OASL, indicating the gene's likely role in non-lytic clearance [28]. Additionally, other cell types have also

demonstrated a reliance on OASL to combat viral infection. Porcine kidney cells transfected with OASL expression vectors demonstrated increased viral defense due to increased OASL activity [60]. Furthermore, it has been experimentally determined that mice with reduced OASL expression are more prone to IAV infection [12]. Overall, OASL plays a clear antiviral function during IAV infection in multiple cell types including club cells, and its role in non-lytic clearance is of interest.

### *HERC5*

HERC5, an E3 ligating protein, is induced by several innate response molecules including TNF- $\alpha$ , pro-IL-1, and type I IFNs, and has demonstrated potent antiviral activity against a number of viruses including SARS-CoV-2, human immunodeficiency virus (HIV), hepatitis C virus (HCV), and IAV [40]. Various studies have investigated this antiviral function and have discovered that, in part, HERC5's ability to attenuate IAV infection is due to its association with and regulation of another strong, anti-influenza ISG. Like, HERC5, ISG15 (ubiquitin-like protein, interferon-stimulated gene 15) is an antiviral gene robustly induced by IFN- $\alpha/\beta$  signal transduction during the initial stages of IAV infection, and plays a key role in the inhibition of viral replication [40]. Knockdown studies have demonstrated that during IAV infection, both HERC5 and ISG15 are critical for IFN- $\alpha/\beta$ -induced antiviral responses [52, 36]. The direct interactions between HERC5, ISG15, and IAV appear to be essential for this effect (**Figure 5**).

Once viral infection is detected in the cytoplasm by PRR's such as RIG-I, ISG15 is rapidly expressed and transferred through a series of host proteins (UBE1L and UBE2L6) prior to conjugation to both viral and cellular proteins [52, 26]. First, ISG15 binds to E1 ubiquitin-like modifier activating enzyme, UBE1L, in an ATP-dependent mechanism. Then, ISG15 is sequentially transferred from UBE1L to UBE2L6, and lastly to HERC5, which binds to ISG15 at the HECT domain found at the C-terminus of HERC5. Once associated with HERC5, ISG15 is stereochemically situated to stably bind with viral proteins, which results in covalent isopeptide bonds between the C-terminus of ISG15 and the  $\epsilon$ -amino group of lysine residues of viral proteins, such as NS1, that are bound to the N-terminus of HERC5, which forms a viral substrate interaction domain. The formation of the covalent bond between ISG15 and the viral protein target inhibits viral protein function as well as prevents protein import into the host nucleus. Pulldown assays and immunoprecipitation analyses have demonstrated that HERC5 attaches ISG15 to several lysine residues on NS1 (K20, K41, K217, K219, K108, K110, and K126). It is now known that ISG15, UBE1L, UBE2L6, and HERC5 are all expressed through the IFNAR-activated JAK-STAT signaling pathway, and in concert, promote ISGylation of viral proteins, which interferes with both their translation during replication as well as their various, subsequent activities during infection [40, 11].



**Figure 7: HERC5 plays a critical role in the ISGylation of viral proteins.** ISG15 is strongly induced during IAV infection. ISG15 is transferred from UBE1L to UBE2L6 and finally to HERC5. Once associated with HERC5 at the HECT domain, HERC5 catalyzes the conjugation of ISG15 to viral proteins bound to HERC5 at the substrate interaction domain at the N-terminus, which results in covalent isopeptide bonds between the C-terminus of ISG15 and the  $\epsilon$ -amino group of lysine residue on viral proteins, thereby inhibiting viral protein function. Created with BioRender.com.

ISGylation, covalent protein-protein interactions between the HERC5-ISG15 complex and IAV proteins, disrupts key elements of viral replication and modulates the innate response to infection through various stages of infection. Early on, this host protein complex's interaction



with viral protein NS1 is known to prevent the nuclear import of vRNPs. As the infection continues and viral mRNA is released into the cytoplasm for translation, ISGylation has been observed to further stall viral replication by inhibiting protein translation as well as blocking post-translational modifications of viral proteins, such as the prevention of the homodimerization of NS1 [40, 36]. As previously discussed, NS1 interacts with protein kinase R (PKR), which prevents several critical antiviral mechanisms from occurring. However, HERC5-ISG15 attachment to NS1 can also inhibit the viral protein's ability to interact with PKR, thereby allowing PKR to function in its normal antiviral role [40]. By the later stage of infection, ISGylation is thought to prevent IAV capsid formation [52].

In addition to interactions with viral proteins, HERC5-ISG15 impacts a variety of cellular proteins during infection as well. Although ISG15 is a ubiquitin-like protein, it does not promote protein degradation. Instead, ISGylation is known to act as a positive regulator of more than 100 ISGs and antiviral genes during the early stages of infection as well as stabilizing key antiviral host proteins during this period [59]. Later, as the viral infection becomes controlled by the innate response, ISGylation is also thought to reduce the expression and stability of some host immunoproteins to reduce inflammation-induced damage, which may prevent cell death in the form of pyroptosis [52, 40].

In a combinatorial effect with ISG15, HERC5 plays a clear antiviral role during influenza infections. ISGylation conjugates with both viral and host proteins, and in doing so, inhibits viral protein mechanisms while at the same time enhances the cell's ability to express and activate additional antiviral genes. These additional genes, along with HERC5, may be critical to non-lytic IAV clearance in club cells.

## *Study goals*

Influenza virus infections are a significant cause of morbidity and mortality globally. Throughout the viral replication cycle, IAV is able to overcome and overwhelm the antiviral defenses of nearly all cells it infects. Club cells in the respiratory system, as an exception to this rule, are capable of non-lytically clearing IAV and continuing to persist after direct infection. The ability of club cells to maintain DNA MMR activity in order to repair their genomes from oxidative DNA damage allows them to fully express key antiviral genes, thus promoting non-lytic clearance. However, the exact genes required for the actual clearance steps are currently unclear. By reviewing the existing literature, we have determined two candidate genes that we hypothesize are critical to non-lytic clearance of IAV in club cells: HERC5 and OASL

By knocking down these genes with siRNA we have evaluated the importance of each gene during the non-lytic clearance of IAV. Using western blots, we confirmed the knockdown of each target gene and subsequently challenged the altered cell lines with Cre-IAV. By performing western blots on collected cells, we evaluated and compared the levels of viral protein HA in knockdown cell lines against untransformed cells. These methods in concert have provided us with the ability to determine the significance of each gene as it applies to non-lytic clearance.

Determining the genetic basis of non-lytic clearance has many potential benefits both in furthering our understanding of the complex interactions between IAV and ISGs, as well as clinical uses. ISGs represent one of the first barriers that IAV must overcome to establish an effective infection. By obtaining a deeper understanding of these ISGs, a clearer picture on how

viral infections can be repelled can be established. Furthermore, results obtained from this study may help explain how other cell types could potentially survive infections using non-lytic viral clearance. From a clinical perspective, new insights into the molecular pathogenesis and cellular antiviral response are invaluable when designing novel antiviral treatments. By identifying key host antiviral genes, future research could potentially investigate their viability in the development of new antiviral therapeutics. Based on our understanding of non-lytic clearance of IAV in club cells, we can hopefully one day increase the survival of other cells and improve the overall outcome of the infected host.

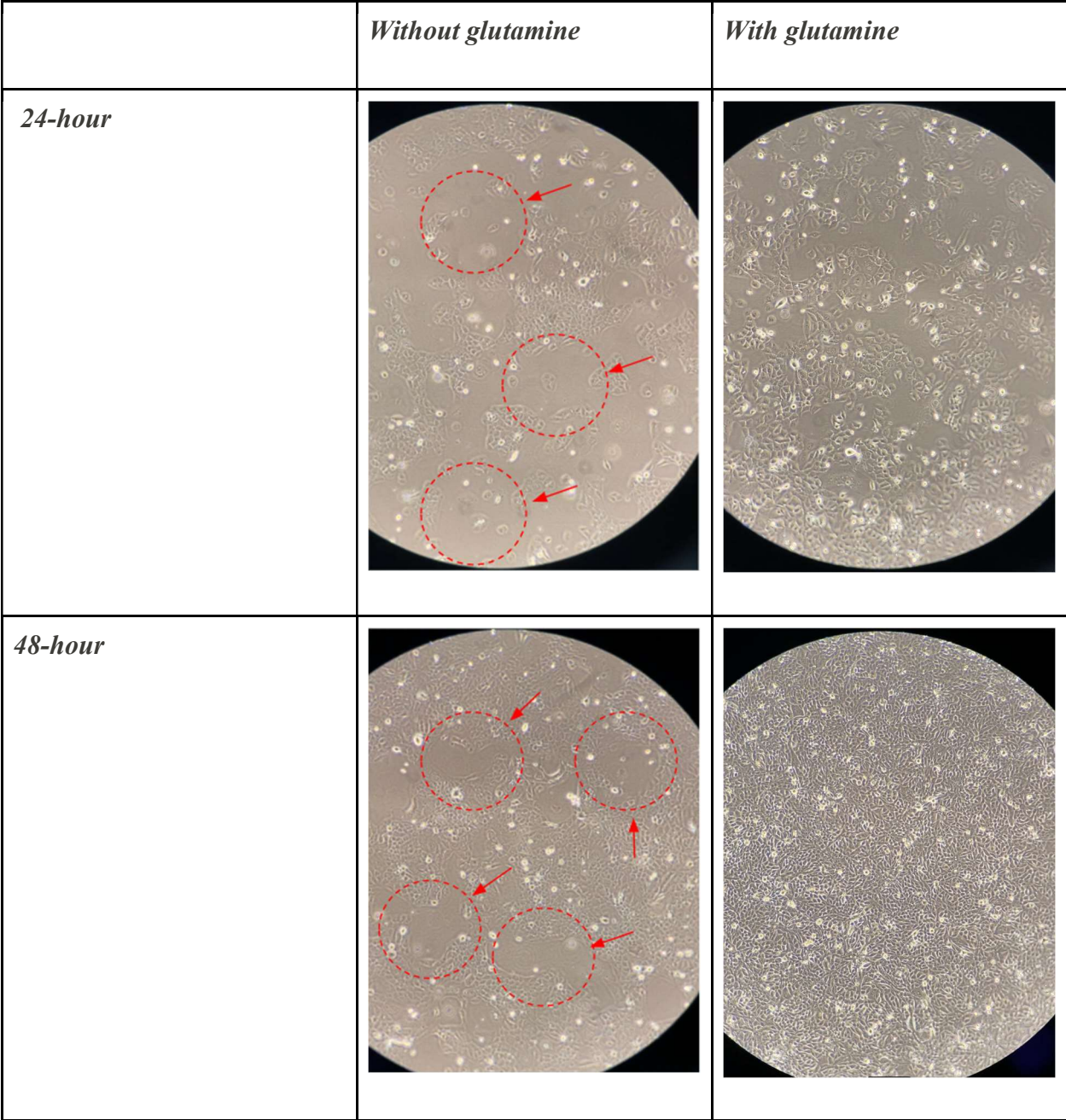
## Results

### *Cell Plating Optimization*

To assess the function of HERC5 and OASL during the clearance of IAV from club cells, we first established a reliable methodology of culturing H441-CR cells (Cre-reporting club cells) in order to grow cell populations for study. Initially, H441-CR cells were grown in 75 cm<sup>2</sup> flasks with RPMI media supplemented with FBS, glucose, HEPES, sodium pyruvate, and penicillin-streptomycin. During our initial cell culturing attempts, the H441-CR cells were observed to be growing at a slower rate than expected, did not form contiguous populations, and did not reach optimal confluence in the flask prior to the media becoming exhausted. Because club cells are epithelial cells, their ideal growth pattern is characterized both by adhesion to a surface, in our circumstance at the bottom of the flasks, as well as cohesion to other club cells. Since our club cells, in addition to growing slowly, were not forming populations that covered the flask bottom in an uninterrupted manner, we determined that our media was potentially not fully optimal for H441-CR growth. To address this suboptimal growth pattern, the media was further supplemented with glutamine, an amino acid with several critical biochemical functions. Previous research has determined the significance of providing an external source of glutamine for the use in mammalian cell culturing. Although glutamine is a non-essential amino acid, many mammalian cell types do not proliferate as quickly or healthily without the supplementation of glutamine in cell culture media, which is quickly scavenged by rapidly growing cells in culture. Biochemical research has indicated that this increased supply of glutamine provides cultured cells with an additional source of carbon and nitrogen for the synthesis of many downstream metabolites as well as playing a role in regulating overall cell biosynthesis and gene expression

[58]. By continuing to grow and passage cells with and without glutamine, we were able to evaluate the effect of this additional supplement over time after each cell flask splitting event **[Figure 8]**.

At 24-hours post-cell split, we observed that cells grown without glutamine lagged behind in confluence when compared to the cells grown with supplemental glutamine and were characterized by patches of low to no cell growth (indicated by dashed circles). At 48-hours, this trend continued, and the cells grown without glutamine were observed to grow in patches and had not reached full confluence. However, the cells grown with glutamine had evenly covered the entire flask surface, become 100% confluent, and were at an ideal stage to be re-split or plated for further experimentation. By determining this result, we were able to amend our culturing protocol and produce healthier H441-CR cell populations in a decreased timeframe.

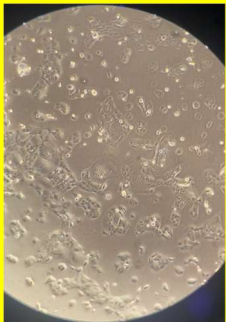



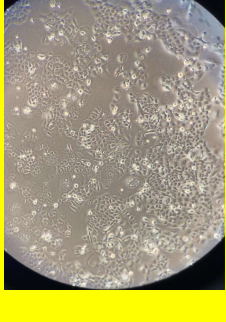

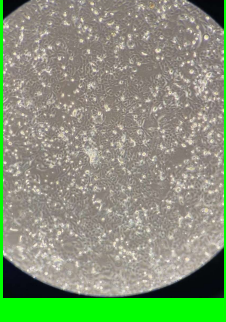
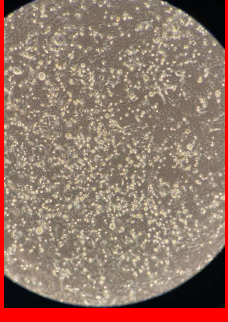

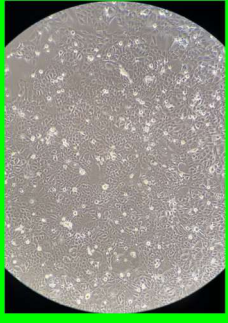
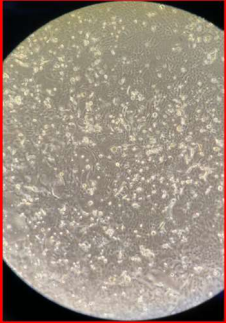



**Figure 8: Optimization of cell culture media.** Flasks of H441-CR populations were grown in RPMI media both with and without supplemented glutamine. Flasks were imaged under light microscopy (100x) at 24-hour, 48-hour, and 72-hour timepoints. Healthy, live cells can be observed growing in clusters that adhere to the plastic flask. Dead cells are characterized by

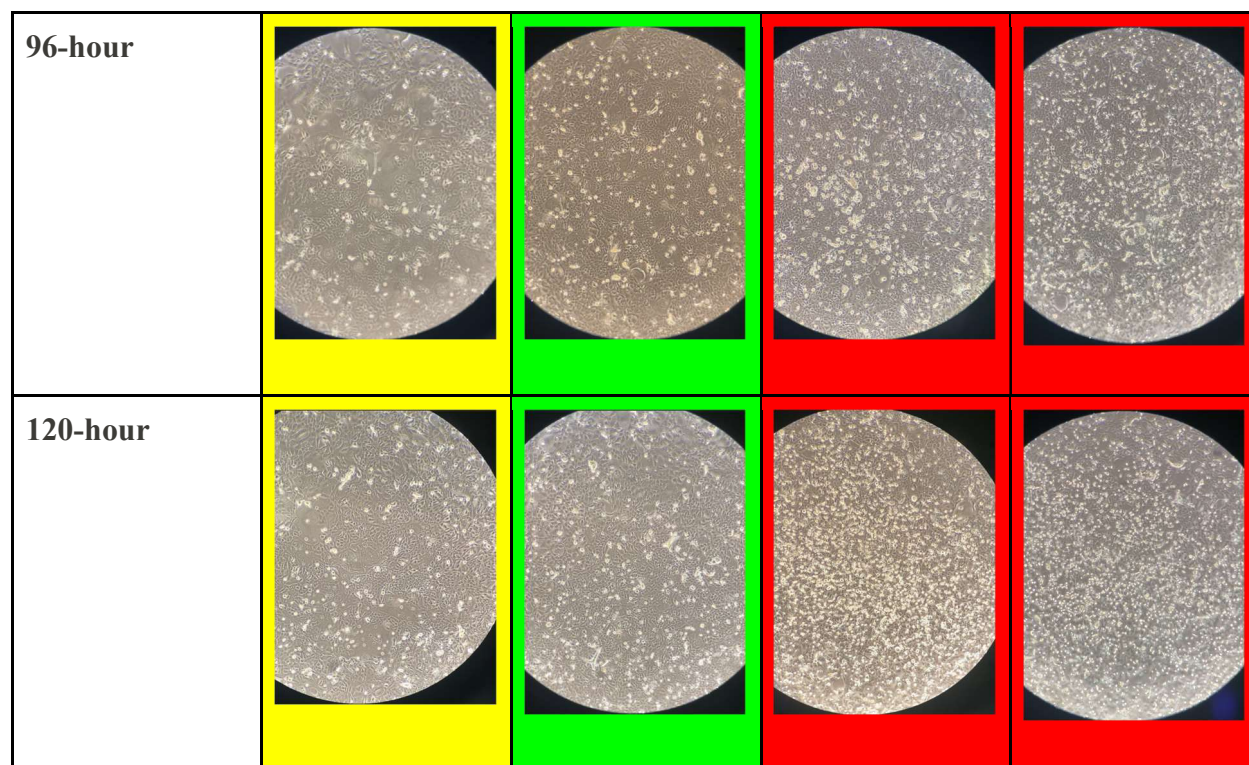
circular shape and have detached from the surface of the plastic. Arrows/dashed circles indicate locations of gaps in the cell layer.

After H441-CR cell populations were confluent and ready for collection and experimentation, the cells were plated in 24-well tissue culture plates. In order to plate the cells to optimal levels for both the transfection and transfection steps, evaluation of the ideal plating concentration was necessary. Club cells grow slower than typical cell lines, thus making the suggested plating concentrations for 24-well plates inaccurate. To determine the optimal plating density of our H441-CR cells, we evaluated four different initial plating densities:  $0.6E5$  cells/well,  $1.2E5$  cells/well,  $1.8E5$  cells/well, and  $2.4E5$  cells/well. These populations, which were not transfected or infected for the purposes of this experiment, were imaged over time to determine which density produced optimal cell confluency for the subsequent steps in future experimentation, transfection, infection, and post-infection sampling [**Figure 9**]. Ideally, cells are transfected 24-hours after plating at an approximately 60-70% confluence. After transfection, the cells are ideally infected 48-hours after plating at approximately 90-100% confluence. The cells were then observed at 24-, 48-, and 72-hours post-infection (equating to 72, 96, and 120 hours after plating). Because H441-CR cells begin to die off from non-viral related conditions when the cells become over-confluent (after 100% confluency has been reached), sub-optimal plating densities can be determined by the presence of an abundance of dead cells. Dead cells, which detach from the bottom of the flask, can be observed by their characteristic circular shape and brighter appearance under light microscopy due to their free-floating nature in the media.



	0.6E5 cells/well	1.2E5 cells/well	1.8E5 cells/well	2.4E5 cells/well
24-hour				
48-hour				
72-hour				





**Figure 9: Optimization of cell plating density.** 24-well plates of H441-CR populations were plated at four densities (0.6E5 cells/well, 1.2E5 cells/well, 1.8E5 cells/well, and 2.4E5 cells/well). Plates were imaged under light microscopy (100x) at 24-hour, 48-hour, 72-hour, 96-hour, and 120-hour time points. Healthy, live cells, which are characterized by amorphous shape, can be observed growing in interconnected populations that adhere to the plastic flask. Dead cells are characterized by circular shape and have detached from the surface of the plastic. Yellow background indicates lower-than-optimal confluence. Green background indicates optimal confluence. Red background indicates over confluence and substantial levels of cell death.

At the 24-hour time-point, we observed for wells plated at 0.6E5 cells/well that confluency was far less than 60% and would not be optimal for transfection. However, the cells plated at 1.2E5 cells/well reached approximately 60% confluency at this time-point, which was

our target confluency for transfection. The wells plated at  $1.8E5$  cells/well had reached  $>60\%$  confluency by the 24-hour time-point, and while these cells would be suitable for transfection, we later observed that this density caused significant cell death due to over-confluence by later time-points. When plated at  $2.4E5$  cells/well, we observed that the cells had already reached 100% confluency by 24 hours and relatively higher cell death is observable when compared to the other plating densities.

At the 48-hour time-point, we observed that the wells plated at  $0.6E5$  cells/well had reached approximately 60%, which is less than the optimal 90-100% confluency target for infection. Those plated at  $1.2E5$  cells/well were observed to have reached an ideal 90% confluency. Wells plated at  $1.8E5$  cells/well had reached full, 100% confluence by 48-hours and a relatively higher amount of cell death was observable when compared to the wells plated at  $1.2E5$  cells/well. Wells plated at  $2.4E5$  cells/well continued to show a significantly higher quantity of dead cells compared to lower plating densities.

At the 72-hour time-point, the wells plated at  $0.6E5$  cells/well had failed to meaningfully increase in confluence and were characterized by non-interconnected groups of cells. The wells plated at  $1.2E5$  cells/well had reached approximately 100%; however, limited cell death was observed when compared to the higher plating densities at the 48-hour time-point. This demonstrated that collecting infected cells plated at  $1.2E5$  cells/well at this time-point would yield a sample primarily containing live, infected cells. The wells plated at  $1.8E5$  and  $2.4E5$  cells/well continued to show significantly higher levels of dead cells due to over-confluence at this time-point.

At the 96-hour time-point, the results continued to show the same trends as prior observations. Wells plated at  $0.6E5$  cells/well had failed to become fully confluent and areas of no cell growth are still observable. The wells plated at  $1.2E5$  cells/well continued to be characterized by full confluence and limited cell death, which indicated that samples of infected cells collected from wells plated at this density would remain optimal. Similarly to the last time-point, wells plated at  $1.8E5$  cells/well and  $2.4E5$  were characterized by large amounts of dead cells caused by over-confluence.

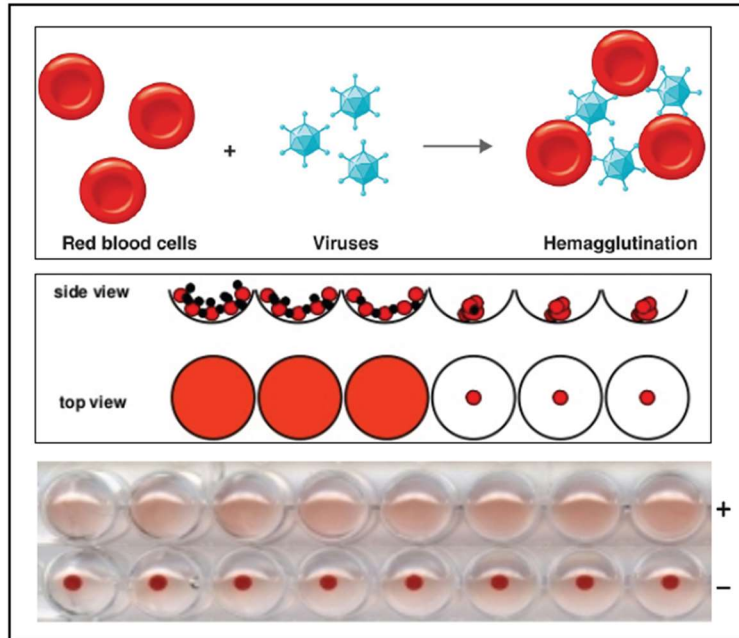
At the final, 120-hour time-point, we observed that the wells plated at  $0.6E5$  cells/well had reached approximately 90% confluence; however, this was achieved 72 hours after the wells plated at  $1.2E5$  cells/well reached a similar point. The wells plated at  $1.2E5$  cells/well were observed to still be relatively healthy and limited dead cells were present particularly when compared to the higher plating densities at earlier time-points. At 120 hours post-plating, the wells plated at  $1.8E5$  and  $2.4E5$  cells/well contained extremely high amounts of dead cells, and the live cells became difficult to observe. This signified that collection of cells from these wells would be less reliable due to the number of cell deaths caused by over-confluence alone.

Through this optimization experiment, we were able to determine the optimal concentration to plate H441-CR cells onto the 24-well plates. Due to the limited media in each well, quick cell growth is ideal; however, growth that is too fast leads to over-confluence and cell death prior to collection. By testing four plating densities, we determined that wells plated at  $1.2E5$  cells/well produced rapid growing H441-CR populations that reach ideal transfection and

infection confluency at the appropriate time-points and did not become over-confluent prior to the collection events.

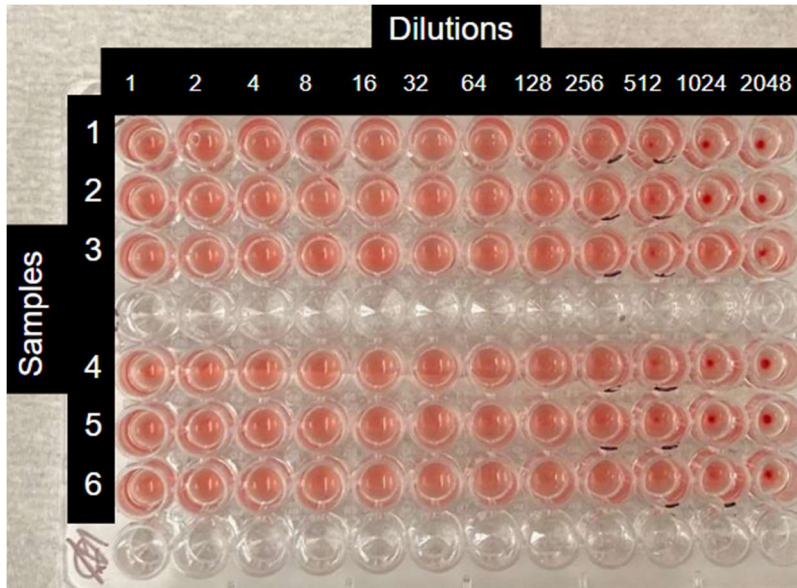
### *IAV Infection Optimization*

In order to assess the criticality of OASL and HERC5 in the clearance of IAV from club cells, we next optimized our methods of infecting the grown H441-CR cells. PR8-Cre IAV virions were initially grown in fertilized chicken eggs to produce a sufficient number of virions for our planned experimentations. To verify that the IAV virions were effectively produced, we performed a hemagglutination assay. The binding interaction between the IAV protein HA and the sialic acid residues on the surface of the red blood cells results in hemagglutination. The lack of IAV virions results in the clumping of red blood cells (RBCs) due to gravity, which is observable to the naked eye [**Figure 10**].



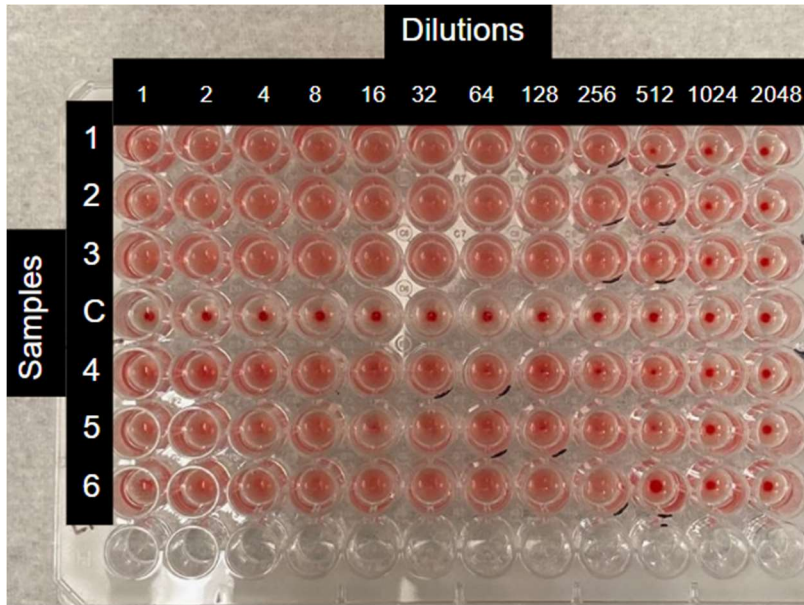
**Figure 10: Presence of hemagglutinin prevents pelletization of turkey red blood cells.** In the top row (+), the binding interaction between influenza virus HA and the sialic acids on the surface of the red blood cells results in hemagglutination. In the bottom row (-), the lack of influenza virus results in the red blood cells pelleting at the bottom of the V-shaped wells due to gravity. (Source: Heaton Lab, Duke University)

During our evaluation, we produced serial dilutions (1:1, 1:2, 1:4, 1:8, 1:16, 1:32, 1:64, 1:128, 1:256, 1:512, 1:1024, and 1:2048) of PR8-Cre virions in PBS and treated wells filled with turkey blood to determine the presence of IAV [Figure 11]. A control row of turkey blood treated with pure PBS was also included [Figure 12]. We observed on average no cell clumping from the 1:1 dilution to the 1:256 dilution, which indicated the IAV virions were successfully grown in the fertilized chicken eggs and were suitable for our infection protocol.




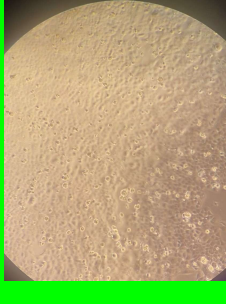
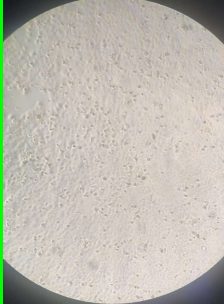
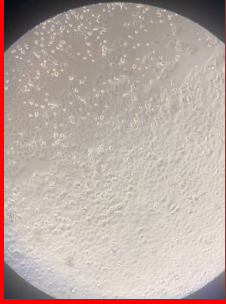
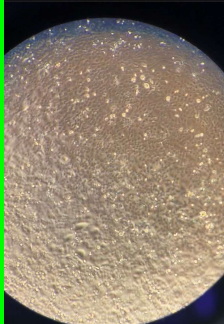
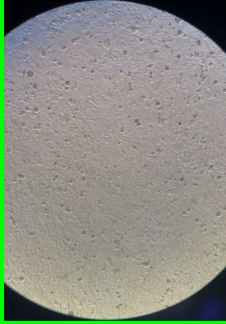


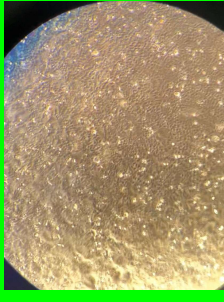
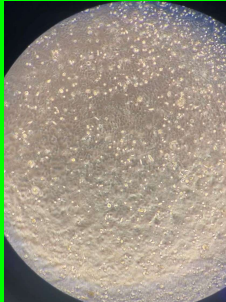
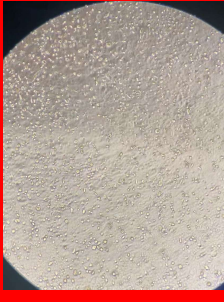

**Figure 11: Hemagglutination assay (HA) results from PR8-Cre viruses grown in fertilized chicken eggs.** Per the protocol described below, an HA assay was performed. Results indicate positive presence of virus (lack of red blood cell pelletization) at all PR8-Cre/PBS dilutions from 1:1 to 1:256. Control dilutions are shown below (Figure 10b).





**Figure 12: Hemagglutination assay (HA) results (with control included) from PR8-Cre viruses grown in fertilized chicken eggs.** Results indicate the presence of virus in all PR8-Cre/PBS dilutions from 1:1 to 1:128. The control sample (PBS only) in Row 4 demonstrates the pelleting of red blood cells in every well.

Once we had determined that we had successfully produced viable quantities of PR8-Cre IAV, we began experiments to optimize the concentration of IAV to challenge the 24-well plated H441-CR cells. The concentration of virions used in an infection treatment is referred to as the Multiplicity of Infection (MOI), which represents the ratio of virions to cells. Based on prior research, we selected and evaluated four different MOIs: 0.1, 0.2, 0.5, and 1.0. H441-CR cells, which were plated at the optimal  $1.2 \times 10^5$  cells/well in 24-well plates, were infected with these different viral concentrations and observed over a 72-hour time-period [Figure 13].

	0.1 MOI	0.2 MOI	0.5 MOI	1.0 MOI
24-hour				
48-hour				
72-hour				

**Figure 13: Infection optimization.** H441-CR cells in 24-well plates were infected with four MOIs. (0.1, 0.2, 0.5, 1.0). Cells were imaged under light microscopy (100x) at 24-hour, 48-hour, and 72-hour timepoints. Healthy, live cells can be observed growing in clusters that adhere to the plastic flask. Dead cells are characterized by circular shape and have detached from the surface of the plastic. Green background indicates a healthy cell population with limited cell death. Red background indicates a cell population with substantial levels of cell death.



At the 24-hour time-point, cells infected at 0.1 MOI were observed to be healthy and relatively higher cell death was not observed when compared to their uninfected counterparts [Figure 9]. Similarly, cells infected at 0.2 MOI were observed to be equally healthy and no excess cell death was detected. Cells infected at 0.5 MOI were relatively healthy compared to their counterparts challenged at lower MOIs; however, a slight increase in cell death was observable compared to the cells infected at 0.1 and 0.2 MOI. Cells infected with 1.0 MOI had begun to show signs of relatively higher cell death at the 24-hour time-point, and areas of cells devoid of healthy cells were present. This indicated already that the 1.0 MOI was likely too high of a viral concentration, and the extreme viral load was overcoming the club cell's ability to resist and clear the virus.

At the 48-hour time-point, the cells infected at 0.1 MOI remain healthy and limited cell death is observed indicating that this concentration was not overwhelming the cells. Similarly, the cells infected at 0.2 MOI continued to appear healthy and no suboptimal amount of cell death was observable. However, cells infected with 0.5 MOI had begun to demonstrate higher levels of cell death and areas devoid of healthy cells began to be observable. Cells infected at 1.0 MOI continued to appear overwhelmed and a significant amount of dead cells were observed in the wells and healthy cells in the wells infected with 1.0 MOI were difficult to observe. At this time-point, both the 0.5 and 1.0 MOI appeared to be too high of viral concentrations for meaningful analysis.

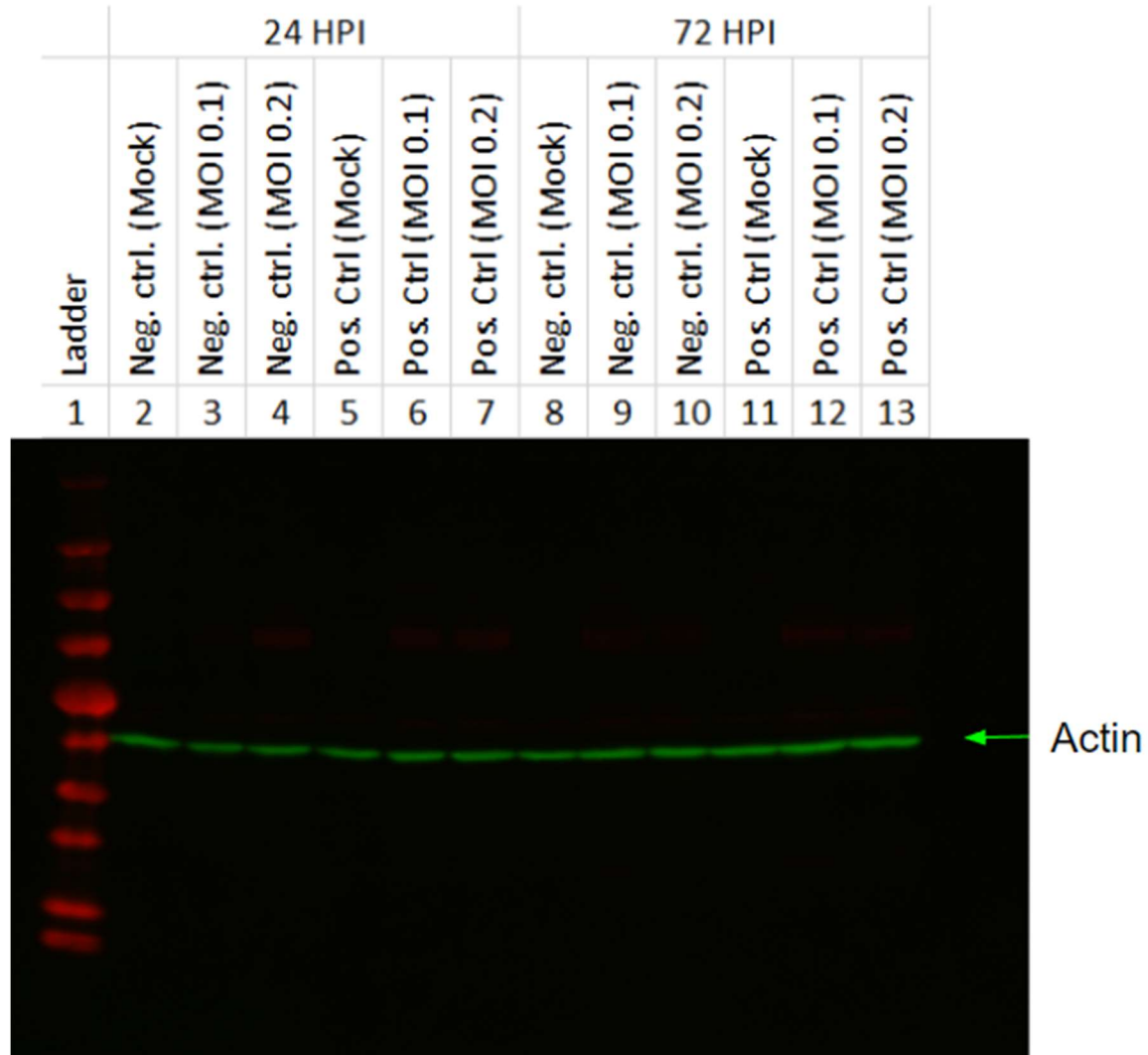
At the 72-hour time-point, the cells infected at 0.1 MOI continued to show limited signs of cell death. Cells infected at 0.2 MOI showed slightly higher levels of cell death; however, the wells remained sufficiently healthy to produce a viable cell collection. Cells infected at 0.5 MOI were observed to have significantly increased in cell death from the previous time-point, and the cells infected at 1.0 MOI appeared to be completely overwhelmed with no readily observable healthy cells.

Determination of the optimal MOI for infection is critical to ensuring that the amount of virus introduced to each cell population is sufficient to both infect the largest amount of cells possible while at the same time not overwhelming the cells to the point where normal viral clearance mechanisms fail. By evaluating four different MOIs, we have determined that both 0.1 and 0.2 MOIs do not overwhelm the H441-CR cells. Since our experimental objective was to infect as many cells as possible, and both 0.1 and 0.2 MOI produced viable, infected populations, we determined that 0.2 MOI is an optimal infection concentration that challenges the largest amount of cells with virus without causing unnaturally high levels of viral load to each cell.

### ***Western Blots***

To evaluate the role of *OASL* and *HERC5* in the non-lytic clearance of IAV from club cells, cells plated in 24-well tissue culture plates were transfected with siRNA for either *HERC5* or *OASL* to achieve a knockdown of protein expression. In order to determine the efficacy of our siRNA knockdown protocol, we initially performed western blots on IAV-infected and mock

infected cell lines transfected with a positive control siRNA or a negative control siRNA to evaluate our experimental controls [Figure 14-15].



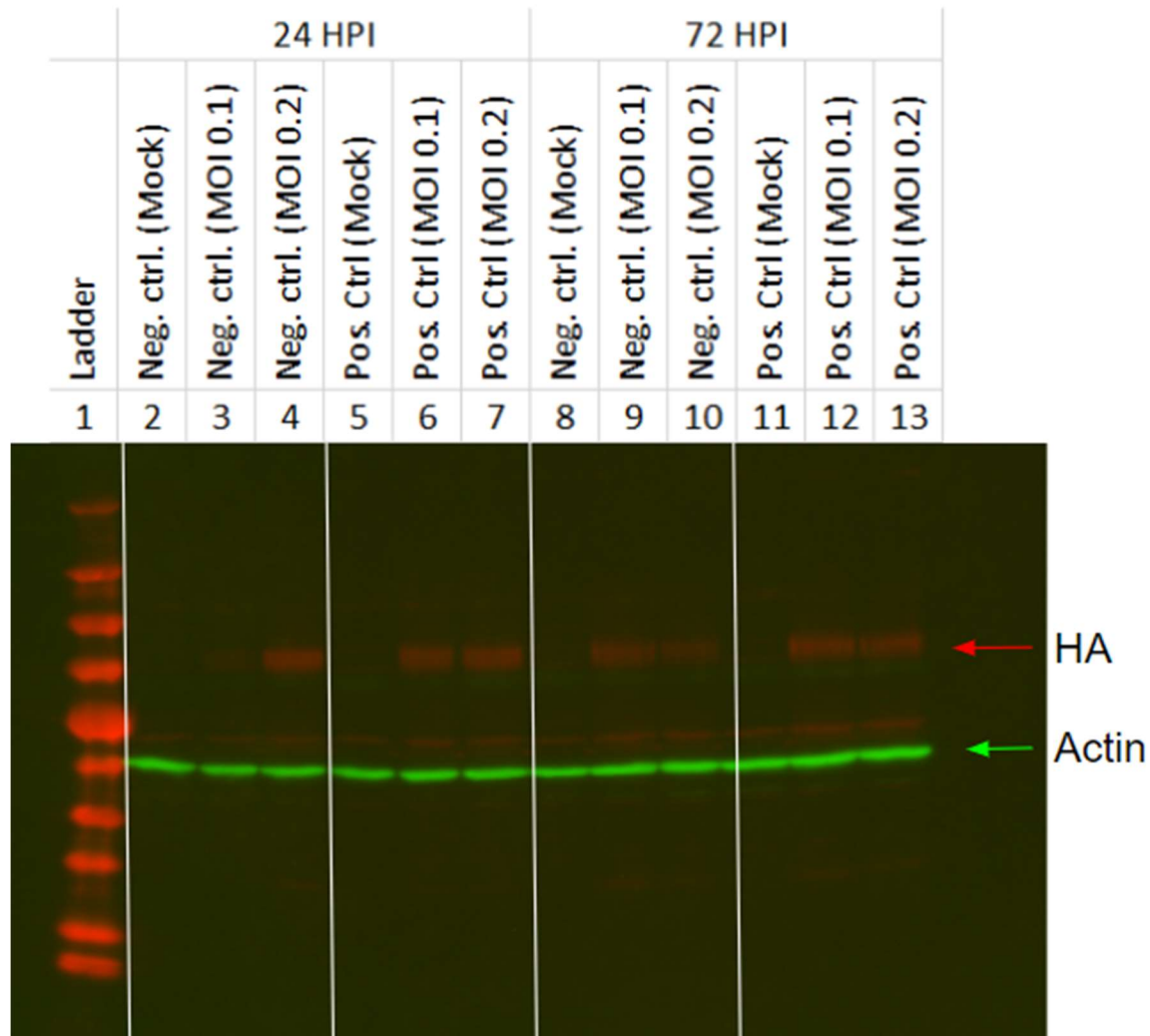
**Figure 14: siRNA control (negative and positive control) evaluation.** H441-CR cells were transfected with negative or positive control siRNA and collected at 24 and 72 hours. Green lateral bands represent the loading control, actin. Consistent actin levels are observable in all lanes.

The positive control siRNA used was specific to the cellular protein JAK1, which is known to play a critical, early role in the immunological response of virally infected cells by inducing the initial cellular signaling cascade for cytokine and ISG expression. The negative control siRNA was an RNA sequence known to have minimal effect on cellular protein expression as there are no known complementary binding sequences in human cells. Each control was evaluated for cells infected with a mock infection, a 0.1 MOI infection, and a 0.2 MOI infection, and samples were collected at the 24hpi and 72hpi time-points. Antibodies specific for the cellular protein actin was used as the loading control.

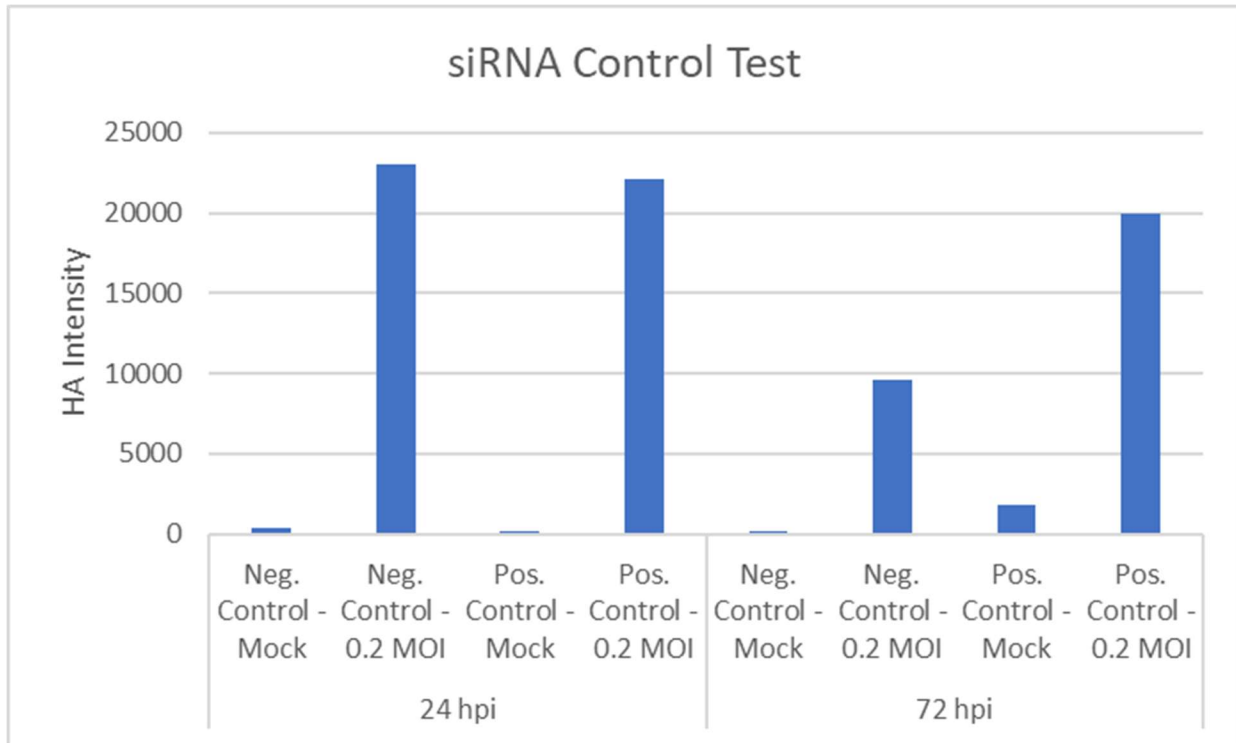
To ensure each well was loaded with an equal amount of collected and prepared sample, we imaged the membrane to highlight the actin quantity in each well **[Figure 14]**. We observed an equal distribution of actin in each well [lanes 2-15] signifying that each well was loaded with a consistent amount of sample.

Next, we imaged the same membrane and increased the visibility of the red bands, which represent the presence and relative quantity of viral protein HA in each well **[Figure 15a-15b]**. We observed that for all samples treated with a mock infection [lanes 2, 5, 8, 11] no HA was detectable. This signified that our mock infection contained no IAV as expected. For all infected samples [lanes 3, 4, 6, 7, 9, 10, 12, 13], HA was observable. Furthermore, our positive control samples [lanes 6, 7, 12, 13] had high HA intensity, which indicated that the knockdown of JAK1 disrupted the cellular immune response as expected. Our negative control lanes [lanes 3, 4, 9, 10] had slightly lower HA intensity, particularly when comparing the 72hpi negative and positive control samples. This indicates that the negative control siRNA did not disrupt the H441-CR cells' ability to begin clearing the IAV infection as was predicted. To note, we observed

relatively lower HA intensity in lane 3. This is potentially due to the lower MOI used on this sample (0.1 MOI), which we previously determined was not the optimal viral concentration.



**Figure 15a: siRNA control (negative and positive control) evaluation.** H441-CR cells were transfected with negative or positive control siRNA and collected at 24 and 72 hours. Green lateral bands represent the loading control, actin. Consistent actin levels are observable in all lanes. Red lateral bands represent IAV protein hemagglutinin (HA). HA is detectable in all infected samples [lanes 3, 4, 6, 7, 9, 10, 12, 13].

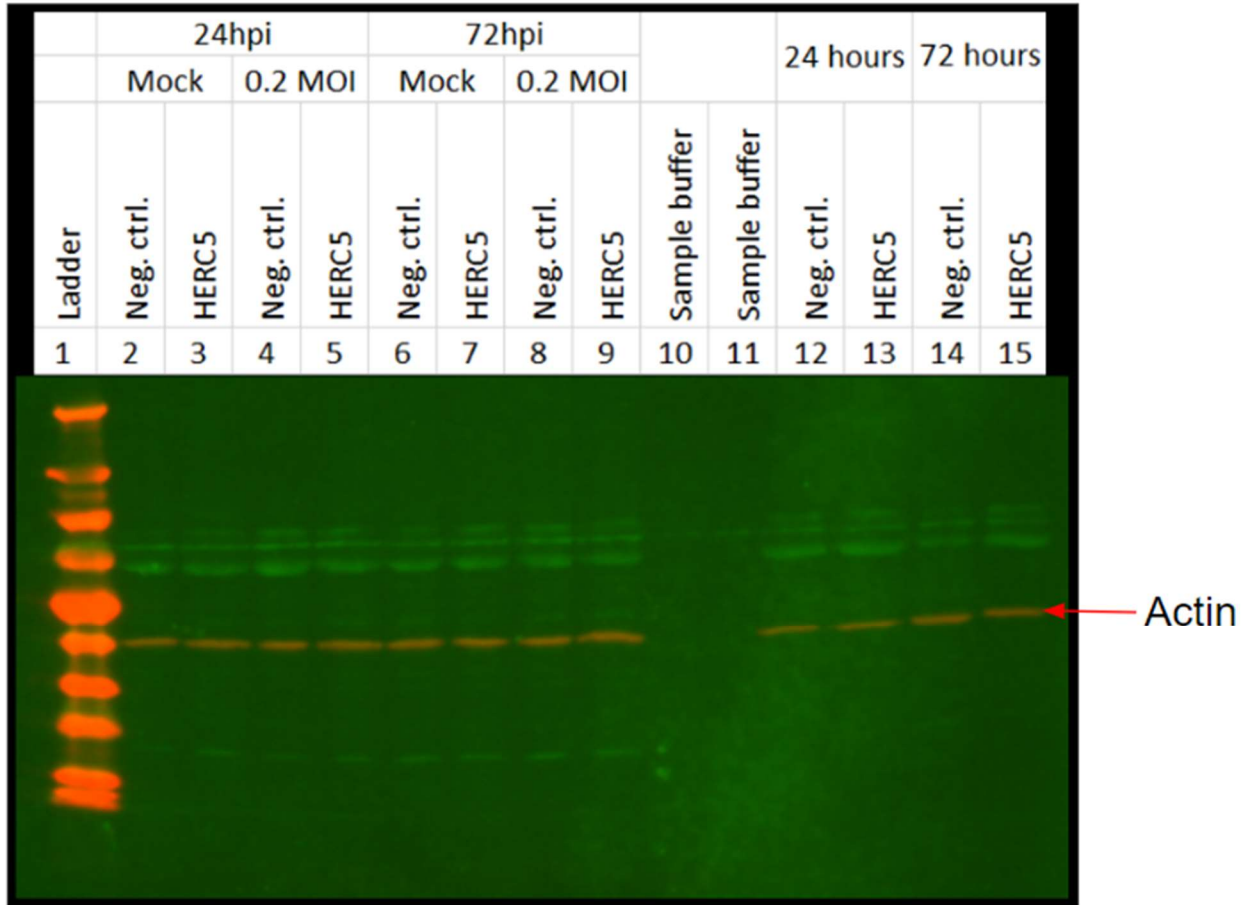


**Figure 15b: siRNA control (negative and positive control) evaluation HA intensity pixel analysis.** H441-CR cells were transfected with negative or positive control siRNA and collected at 24 and 72 hours. HA pixel intensity from western blot (Figure 15a) was evaluated via ImageJ.

By conducting this western blot, we were able to confirm that the mock infection treatment was devoid of IAV, the negative control did not inhibit H441-CR clearance of IAV, and cells treated with positive control siRNA were characterized by relatively higher HA levels (~106% higher HA intensity at 72 hpi) signifying a reduced ability to clear the IAV infection. This demonstrated that our experimental controls for infection and siRNA were effective and produced the desired results.

We similarly performed western blots to confirm the knockdown of both *HERC5* and *OASL*. To confirm *HERC5* knockdown, H441-CR cells were either transfected with negative control or *HERC5* siRNA, treated with a mock infection or 0.2 MOI infection, and collected at 24 and 72 hours. Also, to confirm the knockdown in non-infected cells, additional H441-CR

cells were transfected with negative control or *HERC5* siRNA and were collected after 24 or 72 hours post-transfection [Figure 16].

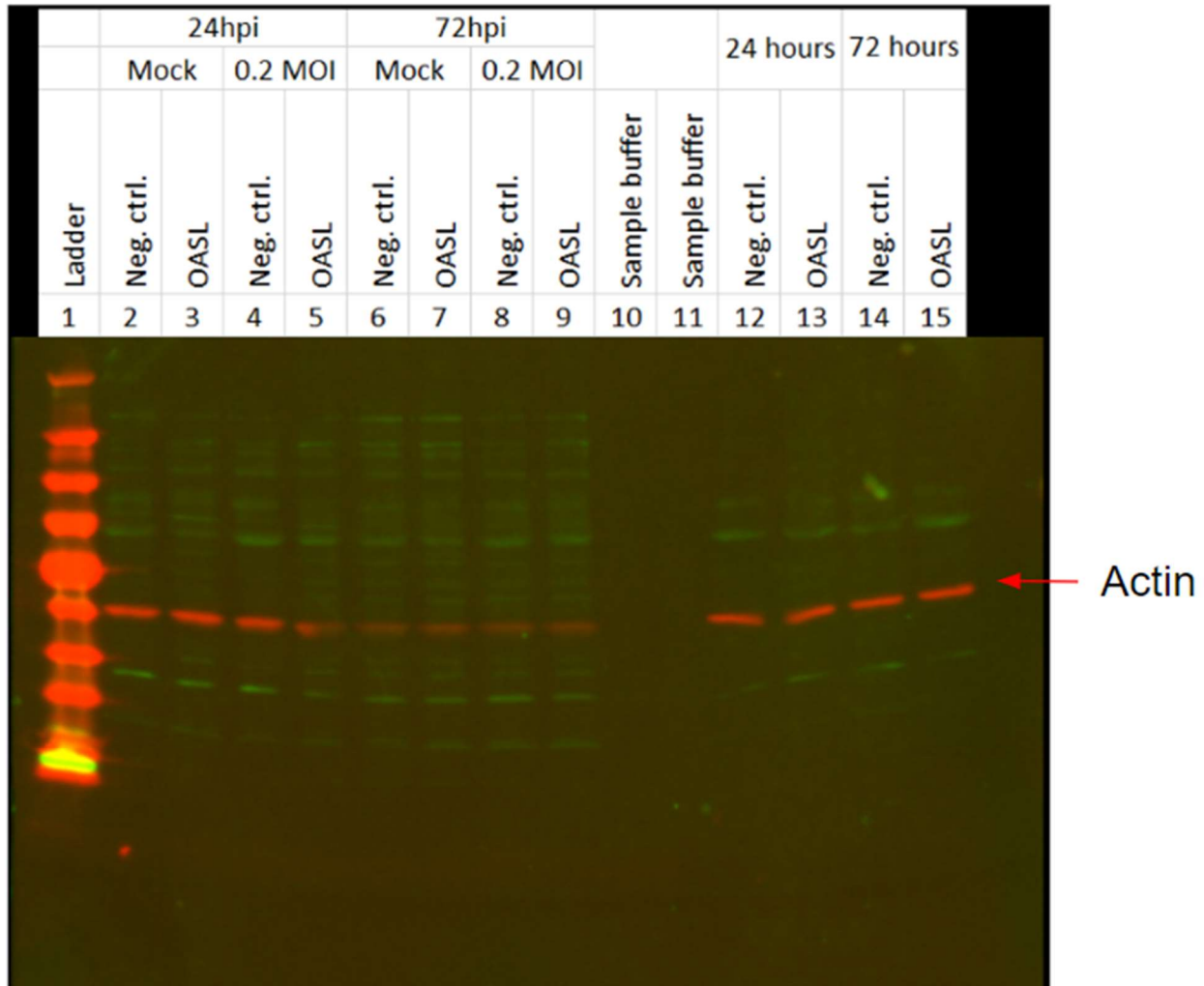


**Figure 16: siRNA confirmation (HERC5).** H441-CR cells were transfected with negative control or HERC5 siRNA, treated with either a mock infection or 0.2 MOI infection, and collected at 24 and 72 hours [lanes 2-9]. Additionally, H441-CR cells were transfected with negative control or HERC5 siRNA and were collected after 24 or 72 hours post-transfection. Red lateral bands represent the loading control, actin. Consistent actin levels are observable in all lanes. Green bands were non-specific and do not reliably represent HERC5 levels in the samples.

Our results from the western to confirm the knockdown of *HERC5* were non-specific and could not be reliably interpreted due to erroneous reporter signaling throughout the membrane. Several issues may have caused these results including an overload of cellular protein in the sample, degradation of the primary antibodies' target antigen, an overabundance of secondary antibodies, and/or the secondary antibodies binding non-specifically in the membrane. However, the siRNA knockdown method and quantities used have previously been confirmed by published research and no signs of cell morbidity were observed after transfection. Several possible steps to correct these results could include adjusting the loading sample amount; however, *HERC5* protein may be expressed in limited quantities and could be difficult to visualize via western blot at lower loading levels. Additionally, alternative secondary antibodies may provide clearer results as the antibodies used may have bound non-specifically to multiple proteins present in the sample. Lastly, different cell lysis techniques may prevent any potential degradation of the *HERC5* antigen. In addition to amending the western blot protocol, alternative techniques such as qRT-PCR could be used to obtain quantitative measurements of cellular mRNA levels of the target gene to confirm successful siRNA transfection.

To confirm *OASL* knockdown, H441-CR cells were similarly either transfected with negative control or *OASL* siRNA, treated with a mock infection or 0.2 MOI infection, and collected at 24 and 72 hours. Additional H441-CR cells were transfected with negative control or *OASL* siRNA and collected after 24 or 72 hours post-transfection to evaluate protein levels in non-infected cells [Figure 17].



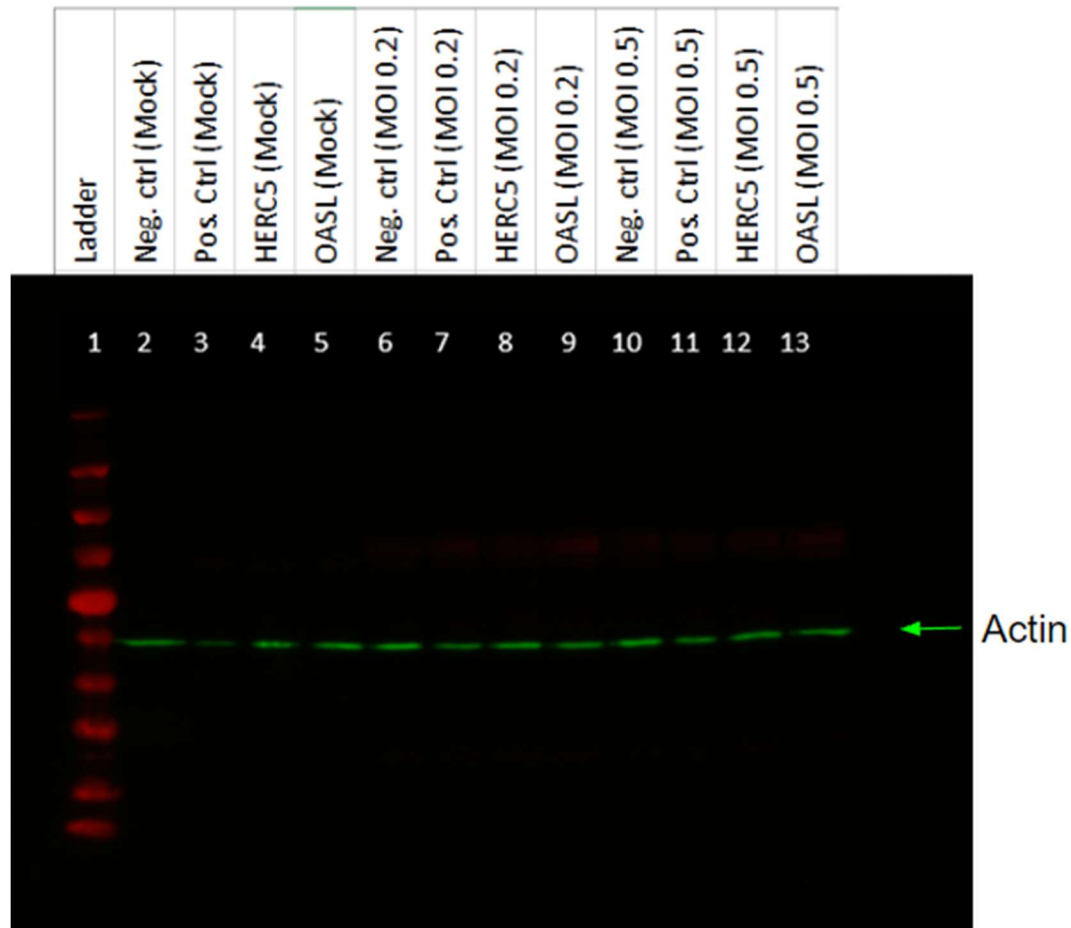


**Figure 17: siRNA confirmation (OASL).** H441-CR cells were transfected with negative control or OASL siRNA, treated with either a mock infection or 0.2 MOI infection, and collected at 24 and 72 hours [lanes 2-9]. Additionally, H441-CR cells were transfected with negative control or OASL siRNA and were collected after 24 or 72 hours post-transfection. Red lateral bands represent the loading control, actin. Consistent actin levels are observable in all lanes. Green bands failed to reliably represent OASL levels in the samples.

Similar to the *HERC5* knockdown confirmation, our results from the *OASL* knockdown confirmation were unreliable due to a non-specific antibody binding in the membrane. We

observed our reporter antibody bands throughout the gel, which again indicated that issues such as an overload of cellular protein in the sample, degradation of the primary antibodies' target antigen, an overabundance of secondary antibodies, and/or the secondary antibodies binding non-specifically in the membrane caused the results to be uninterpretable. Similar amendments to the protocol as stated previously for the *HERC5* knockdown confirmation would be appropriate to apply to this experiment as well in order to obtain viable results.

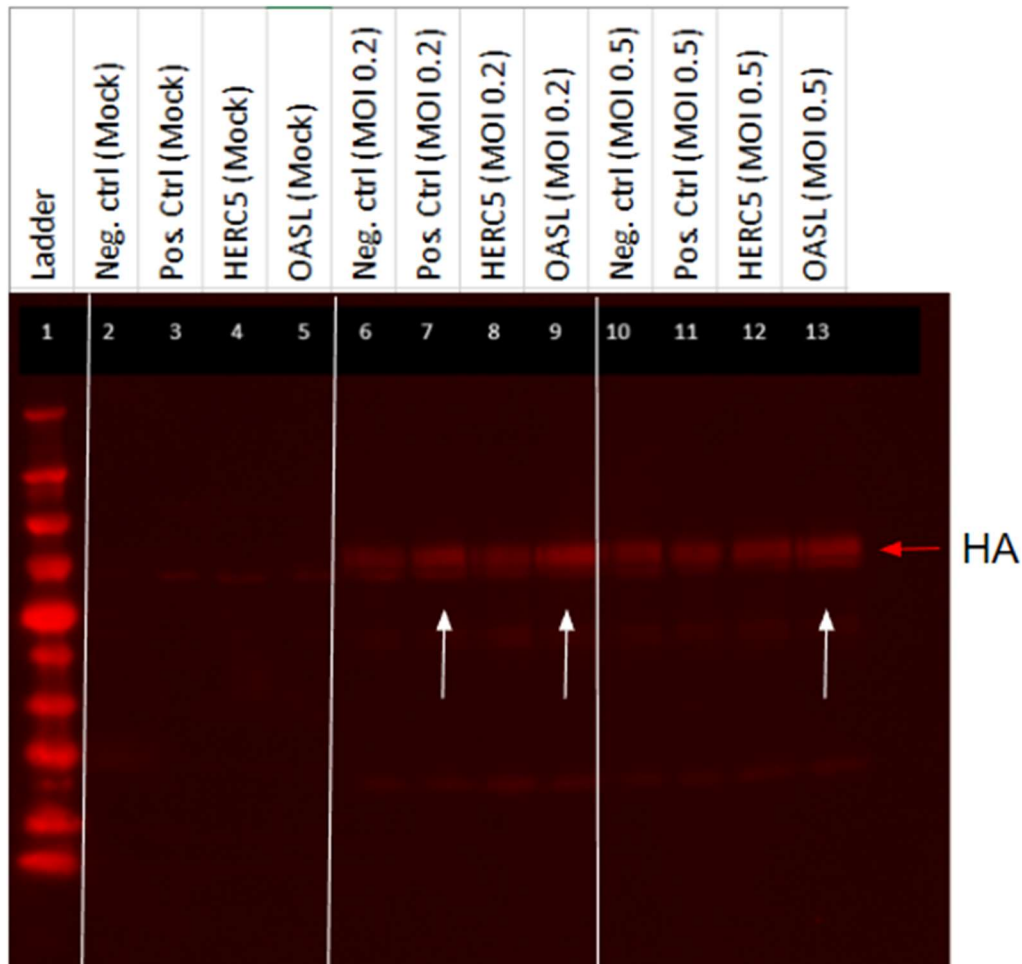
To evaluate our hypothesized role of *HERC5* and *OASL* in the clearance of IAV, we performed a western blot on H441-CR cells transfected with either our positive control, negative control, *HERC5* siRNA, or *OASL* siRNA. Each sample was challenged either with a mock infection, a 0.2 MOI infection, or a 0.5 MOI infection and samples were collected at the 72hpi time-point [Figure 18].



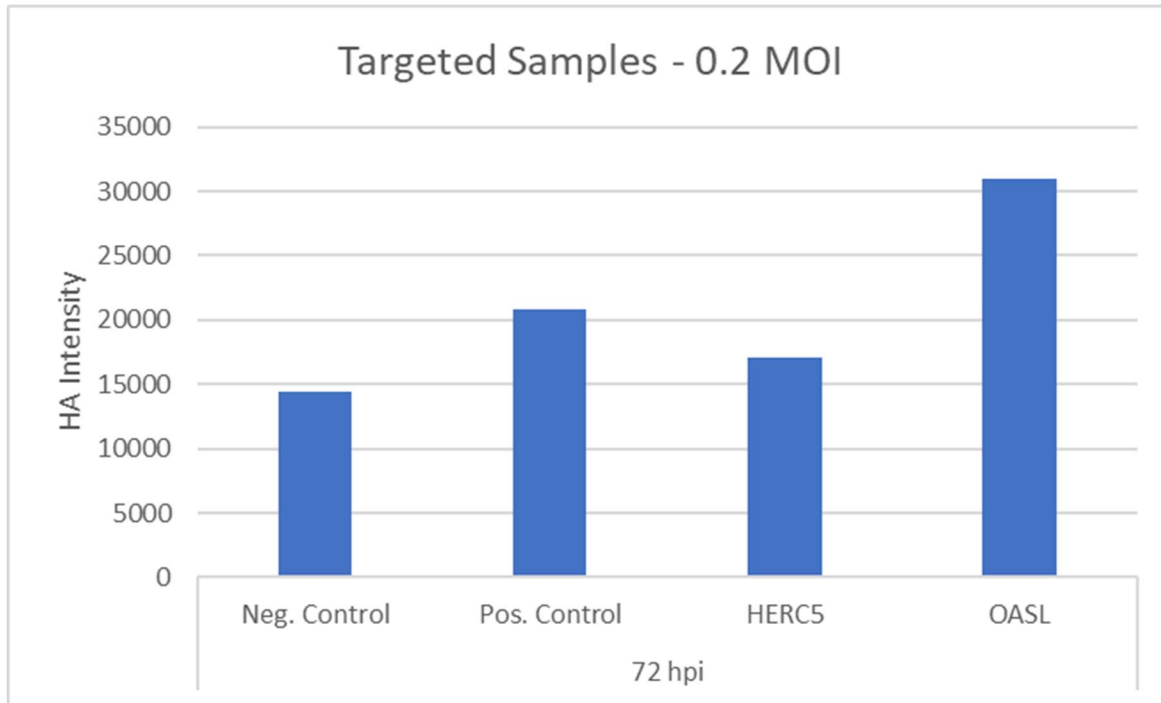
**Figure 18: Targeted gene evaluation (HERC5 and OASL).** H441-CR cells were transfected with negative control, positive control, *HERC5*, or *OASL* siRNA and challenged with IAV (MOI 0.2, 0.5) or mock infection and collected at 72 hours post-infection. Green protein bands represent the loading control, actin. Consistent actin levels are observable in all lanes except lane 3.

Similar to previous westerns, we treated the membrane with antibodies specific for actin to confirm each well was loaded with an equal amount of sample. We observed that all lanes except lane 3 expressed similar levels of actin intensity. Lane 3 had potentially been loaded with less sample amount than the other lanes; however, lane 3 samples were treated with a mock infection and no HA was expected to be detected.

Subsequently, we re-imaged the same membrane to increase the visibility of the red bands, which indicate the presence and relative quantity of HA [Figure 19a-19b]. For the cells treated with mock infection [lanes 2-5], no HA was detected. Cells treated with a 0.2 MOI infection (6-9) all displayed HA in varying intensity. HA levels were observed to be lowest in the negative control (lane 6) and *HERC5* siRNA transfected cells (lane 8). We observed relatively higher HA intensity in both the positive control [lane 7] (~45% higher HA intensity) and *OASL* siRNA transfected cells [lane 9] (~115% higher HA intensity). Higher HA levels in the positive control were expected due to the knockdown of JAK1. The observation of higher HA levels in the *OASL* knockdown cells indicate that the reduced expression of *OASL* may inhibit the clearance of IAV from the cell.



**Figure 19a: Targeted gene evaluation (HERC5 and OASL).** H441-CR cells were transfected with negative control, positive control, *HERC5*, or *OASL* siRNA and challenged with IAV (MOI 0.2, 0.5) or mock infection and collected at 72 hours post-infection. Red lateral bands represent IAV protein Hemagglutinin (HA). Higher HA intensity observable in lanes 7, 9, and 13 (indicated by white arrows).



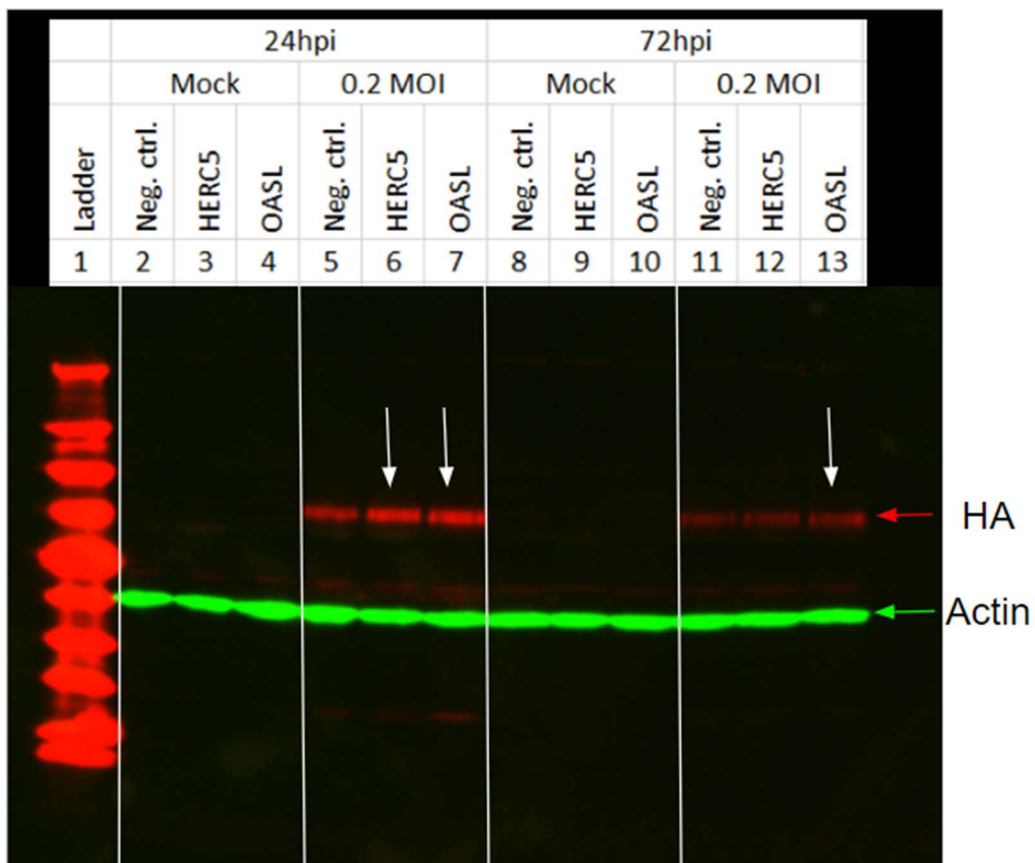
**Figure 19b: Targeted gene evaluation (HERC5 and OASL) HA intensity pixel analysis.**

H441-CR cells were transfected with negative control, positive control, *HERC5*, or *OASL* siRNA and challenged with IAV (MOI 0.2) or mock infection and collected at 72 hours post-infection. HA pixel intensity from western blot (Figure 19a) was evaluated via ImageJ.

Cells treated with 0.5 MOI [lanes 10-13] were observed to show relatively similar results. In particular, the cells transfected with *OASL* siRNA [lane 13] expressed the highest levels of HA further indicating the potential criticality of *OASL* in the clearance of IAV from club cells. The remaining lanes [lanes 10-12] showed relatively equal intensities of HA. As we determined previously, 0.5 MOI was a suboptimal viral concentration, and it is possible that the negative control, positive control, and *HERC5* siRNA transfected cells were equally overwhelmed by this higher concentration of viral infection and no distinction between the three sample types could be determined. This further substantiated our understanding of the optimal infection MOI as well

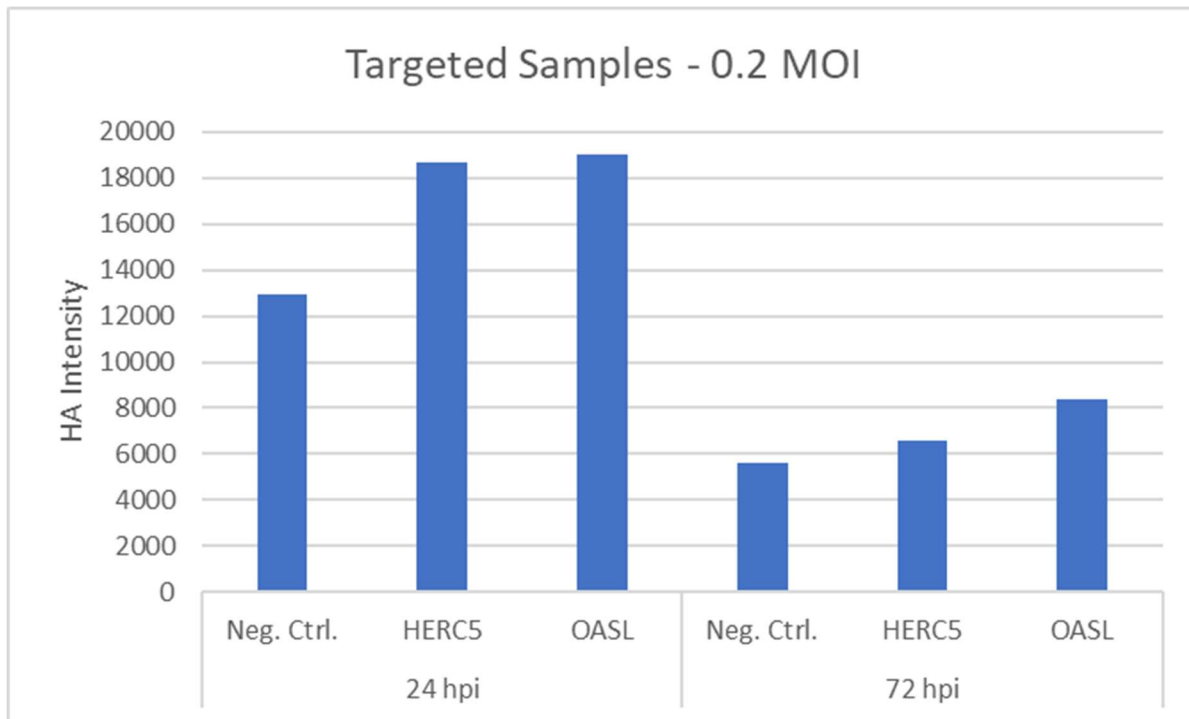
as determined that *OASL* was potentially the most critical gene in IAV clearance of the two target genes evaluated.

To further evaluate our target genes, *HERC5* and *OASL*, we performed an additional western on H441-CR cells transfected with either our negative control, *HERC5* siRNA, or *OASL* siRNA. Each sample was challenged either with a mock infection or a 0.2 MOI infection, and samples were collected at both a 24hpi and 72hpi time-point to potentially track changes in viral protein over time [Figure 20a-20b].



**Figure 20a: Targeted gene evaluation over time (*HERC5* and *OASL*).** H441-CR cells were transfected with negative control, *HERC5*, or *OASL* siRNA and challenged with IAV (MOI 0.2)

or mock infection and collected at 24 and 72 hours post-infection. Green protein bands represent the loading control, actin. Consistent actin levels are observable in all lanes. Red lateral bands represent IAV protein Hemagglutinin (HA). Higher HA intensity observable in lanes 6, 7, and 13.



**Figure 20b: Targeted gene evaluation over time (HERC5 and OASL) HA intensity pixel analysis.** H441-CR cells were transfected with negative control, *HERC5*, or *OASL* siRNA and challenged with IAV (MOI 0.2) or mock infection and collected at 24 and 72 hours post-infection. HA pixel intensity from western blot (Figure 20a) was evaluated via ImageJ.

At the 24hpi time-point, we observed that for all cells treated with a mock infection [lanes 2, 3, 4], no HA was detected. In all cells treated with a 0.2 MOI infection [lanes 5, 6, 7], HA was detectable. Notably, HA levels appeared higher in both the HERC5 (~44% higher HA



intensity) and OASL (~46% high HA intensity) knockdown cells than the negative control, which further substantiates OASL's potential criticality in non-lytic clearance as well as provides evidence that HERC5 may also play a role.

At the 72hpi time-point, we again observed no HA in any cells treated with the mock infection [lanes 8, 9, 10] as expected. Alternatively, HA was observable in all cells treated with a 0.2 MOI infection [lanes 11, 12, 13]. Although the infected cell treated with either the positive control or HERC5 knockdown expressed similar levels of HA, the HA intensity in the OASL knockdown sample [lane 13] was higher (~48% high HA intensity) once again indicating OASL's potential role in IAV clearance. However, it is clearly observable that HA levels in the 72hpi infected samples are all lower than the 24hpi infected samples. This is likely representative of the H441-CR cells' ability to clear the virus over time, although the H441-CR cells transfected with OASL siRNA may not be able to do so as quickly. The diminished rate at which OASL knockdown cells can clear IAV leads us again to the conclusion that our target gene is likely necessary for a club cell's ability to fully and effectively clear IAV.

## Discussion

Unlike all other respiratory cell types, club cells are currently believed to be the only cells capable of non-lytically clearing an active IAV infection. Due to the cell's ability to maintain MMR activity, club cells are able to successfully generate an antiviral cellular state due to the continued expression of antiviral genes, such as ISGs. Of these ISGs, we evaluated both OASL and HERC5 to determine their criticality of these genes in the role of non-lytic clearance individually via siRNA knockdown.

Optimization of several methods was required prior to the analysis of each gene, and here, we analyzed the impact of several alternative approaches to cell culturing, cell plating, and viral infection techniques. Ideal H441-CR cell growth is necessary to create reliably testable populations as well as obtain optimal confluency during transfection, infection, and collection events. After observing suboptimal cell growth with our initial media, we determined that the presence of additional glutamine significantly increases H441-CR health when grown in cell culturing flasks as determined via the evaluation of cell confluence under light microscopy. The observation of healthier populations under a shorter time-frame signified that this amended cell media produced cells more closely resembling healthy club cells in the natural, human body environment and therefore would produce more reliable results when infected.

Furthermore, by determining that the ideal plating density for H441-CR in a 24-well plate is  $1.2 \times 10^5$  cells/well, we were able to produce confluent, healthy populations that would be ready for transfection, infection, and collection at the appropriate time-points. Transfection of plated H441-CR cells is optimal when the cells have reached approximately 60% confluence, and the

optimal confluence for infection is approximately 90-100%. By conducting this optimization experiment, we determined that when plated at  $1.2 \times 10^5$  cells/well, 60% confluence was reached at 24 hours after plating, and 90-100% confluence was reached at 48 hours after plating. This determination ideally coincided with our observation that the siRNA knockdown was most effective 24 hours after transfection, which coincided with our infection time-point. This signifies that the H441-CR cells were infected when the protein expression of our target proteins were at their lowest level, which allowed us to most effectively evaluate the impact of siRNA knockdown on viral protein clearance. However, we also observed that protein expression of our targets began to recover by 48 hours post-transfection as the siRNA degrades. Additional transfection methods such as CRISPR-Cas9 knockout techniques could substantiate these results by permanently decreasing target cellular protein levels.

Additionally, we evaluated several viral MOIs to determine the optimal infection protocol that would enable us to infect as many plated H441-CR cells as possible without overwhelming the individual cells with an unnatural level of virus that would potentially overwhelm the club cell's native ability to clear IAV. Over the course of multiple infection experiments, we determined that the optimal MOI for H441-CR infection was 0.2 MOI. At this level, H441-CR were infected with a sufficiently high level of IAV, which was later substantiated by the presence of HA visible in the western blots performed, as well as low enough to allow non-transfected cells to survive and clear the virus without becoming overwhelmed. The implication of finding this optimal MOI was the ability to infect, as close as possible, the entire H441-CR population in each well while also maintaining cell population viable enough to survive through the 24hpi and 72hpi collection time-points, which provided us with ideal samples of primarily live cells.

Based on our results, we have determined that OASL may play a role in non-lytic clearance. Previous research has determined that OASL is responsible for maintaining the activity of the PPR RIG-I during IAV infection, which is typically suppressed during an IAV infection due to the inhibitory effects of viral protein NS1. By counteracting NS1's inhibitory impact on RIG-I, OASL allows for the detection of cytosolic vRNA in the cell, which releases from the viral capsid prior to nuclear entry. Because of this role, OASL is likely critical in the cell's ability to detect the early stages of viral infection and activate antiviral genes quickly through RIG-I induced IFNs. Previous studies evaluating the loss of OASL expression have indicated that the suppression of OASL leads to the reduction of RIG-I signaling. Although OASL is not thought to play a direct role in neutralizing the virus, a lowered antiviral gene expression would inhibit clearance in general as was observed in non-club cell types due to MMR suppression in past research. Previous work conducted on non-club cell lines has also demonstrated that the expression of OASL leads to the reduced ability of murine parainfluenza virus to replicate in mammalian cells. In our study, we demonstrated that club cells (H441-CR) transfected with OASL siRNA displayed a reduced capacity to clear the virus as indicated by relatively higher levels of HA in the infected cells when visualized through western blot imaging, which implies an increased viral reproduction rate when compared to the negative control. In the context of previous work conducted on OASL, our results are consistent in showing that a reduction in OASL potentially leads to a decreased innate cellular antiviral defense against IAV in club cells.

These results substantiate OASL's potential criticality in non-lytic clearance; however, further evaluation of the proteins role in cellular viral defense against IAV is needed. While western blots allow for the observation of relative protein levels in the cell, other more

quantitative methods could be applied to produce additional confirmations of this role such as ELISA and qRT-PCR. By quantifying the levels of viral protein over time, further investigation can determine the magnitude of impact the knockdown of OASL has on club cells' ability to clear virus over the course of an IAV infection. Additionally, a replication of our study that includes an analysis of RIG-I function and IFN expression may help to tie OASL's role in activating RIG-I to antiviral gene induction in club cells while simultaneously evaluating the overall impact on IAV clearance.

Although the knockdown of OASL appears to reduce the ability of H441-CR cells to clear IAV as quickly as non-transfected cells, it is notable that significant cell death was not observed. Immunological defense against pathogens is in general characterized by redundant mechanisms, and the innate antiviral defense is no exception to this trait of immune defense. Although the scope of this project was limited to two genes, many ISGs with known antiviral activity exist in human somatic cells. Furthermore, with respect to OASL specifically, although OASL may be critical for the activation of RIG-I receptors during IAV infection, other PRRs are capable of detecting the presence of a viral infection and inducing an antiviral state including TLRs and NLRs. So, while we propose that OASL may be critical to clearance of IAV in club cells, if OASL is individually knocked down and all other ISGs are fully expressed, the cell has redundant mechanisms that may allow the cell to survive; however, the clearance of IAV appears to occur at a slower rate and is potentially less effective when the expression of OASL is diminished. Additionally, it is possible that more club cells succumb to IAV when OASL is not expressed, but the analysis of cell death rate was outside the scope of this project and would require further experimentation to confirm. Our results indicate that OASL may be a part of what is likely a complex array of genes necessary to clear IAV, and continued research into other

candidate genes as well as the analysis of synergistic effects of ISGs working in concert is necessary to determine the complete picture of IAV clearance in club cells.

During our evaluation of HERC5, HA levels detected in the western blot from infected cells were primarily observed to be similar to those of the negative control, which indicated that the knockdown of the HERC5 gene alone did not critically impair the H441-CR cells' ability to non-lytically clear the IAV infection. However, in a subsequent replication, HA levels were observed to be slightly elevated in the HERC5 knockdown cells after 24 hours post-infection at 0.2 MOI. Due to the disparity in results, further evaluations should be conducted to clarify whether the absence of full HERC5 expression impacts the ability of club cells to non-lytically clear IAV. Although prior research has demonstrated that HERC5 plays an important role in the cellular defense against viruses by regulating the binding and neutralization of key viral proteins to cellular proteins (ISG15) via ISGylation, our results may indicate that the knockdown of this mechanism doesn't significantly impede viral clearance. However, previous research has determined that the catalytic role of HERC5 in ISGylation is essential to this antiviral mechanism, but many viruses have also adapted strategies to resist HERC5 and ISG15 antiviral activity. Further research on whether IAV is capable of antagonizing HERC5's function in the role of ISGylation would provide valuable insight into whether HERC5 plays a significant role in the non-lytic clearance of IAV in club cells. Whether the low levels of HERC5 present after siRNA knockdown are still sufficient to clear the virus, if ISGylation can be activated by other, redundant cellular proteins, or if IAV is capable of inhibiting HERC5 and ISG15's role in a significant manner remains unknown. Since some data produced during this study indicated a potential increase in IAV replication in HERC5 knockdown cells, further analysis is warranted. Additional methodologies, such as ELISA and qRT-PCR, may provide a clearer picture of

HERC5's impact on viral clearance through the quantification of both HERC5 mRNA and HA levels.

A limitation of this study was due to our experimental design in which each gene was assessed individually. In the context of a natural infection, the innate cellular response is built on the complex, interdependent relationship of many antiviral genes acting in concert. While our study focused on determining the impact of gene knockdown on our targets one by one, further analysis of these ISGs may include the knockdown or knockout of several at the same time to evaluate any potential interdependent function of the candidate genes. Furthermore, our study was limited by the unavailability of MDCK cells, which are commonly used to conduct plaque assays that determine viral titer levels. This enables a more accurate assessment of viral infection concentrations, and with this information, infections mimicking natural infection levels could be more easily achieved.

These data provide rationale for continued research into the role of OASL and HERC5, as well as other known ISGs, during the non-lytic clearance of IAV from club cells. While the mechanism to clear viral infection is a function of many genes, understanding individual gene function and the significance of that function helps further our overall understanding of the innate antiviral response in club cells. Our results indicate that when OASL expression is knocked down, the cell's ability to halt the reproduction of IAV and clear its constitutive proteins is diminished, likely due to an inhibited ability to detect the presence of IAV during the early stages of infection. While similar results for HERC5 were not obtained during this study, our limitations are clear, and continued research using alternative methods and approaches may find data supporting our initial hypothesis. Overall, this study demonstrates the ability to study the

criticality of ISGs in club cells during non-lytic clearance, which may hold significant implications in the future development of antiviral therapies against IAV as well as further our understanding of non-lytic clearance in general. Next steps, including the individual evaluation of other ISGs with suspected roles in non-lytic clearance as well as evaluating the synergistic effect of multiple ISGs via the knockdown or knockout of several genes, present a clear path to reaching this further understanding.



## **Methods**

### *Cells*

The H441-CR (Cre-reporter) cell line used in the study was obtained as a gift from the lab of Dr. Peter Palese at the Icahn School of Medicine at Mt. Sinai. The cells were grown at 37°C in a 5% CO<sub>2</sub> environment. The H441-CR cells were grown in RPMI media and supplemented with FBS, glucose, HEPES, sodium pyruvate, penicillin-streptomycin, and glutamine. All cell cultures were split as needed every 2 or 3 days when cells reached optimal coverage (approximately 80% - 90% confluence) determined by light microscopy. Spent media was removed from flask and flask washed with PBS. Trypsin was added to release the cells from the plastic surface of the flask for splitting. New media was added to flasks during each splitting event or media exchange.

### *Viruses*

The “PR8-Cre” virus strain was obtained as a gift from the lab of Dr. Nicholas Heaton at the Duke University School of Medicine. The PR8-Cre virus contains WT gene segments from the A/Puerto Rico/8/1934 H1N1 influenza virus strain. Recombinant vRNA segment 1 (PB2) was used to express the Cre recombinase gene. The virus was diluted with PBS (1:500) and grown in fertilized chicken eggs obtained from Charles River Laboratories. Virus-infected eggs were incubated for 48-72 hours at 37°C and 45% relative humidity. Virus was extracted from eggs, aliquoted, and frozen at -80°C. To confirm the presence of virus, IAV hemagglutination (HA) assays were conducted. For the HA assay, collected virions were mixed with PBS to create serial

two-fold dilutions in 96-well V-bottom plates containing turkey red blood cells. Agglutination of the red blood cells indicated the presence of viruses.

### ***siRNA Knockdown***

Cells were transfected with siRNA of target genes (*HERC5*, *OASL*) using Lipofectamine™ 2000 and the manufacturer's protocol. Prior to transfection, cells were grown to a minimum of 60% confluence in a 24-well plate. Each transfection sample of Silencer Select™ siRNA (Thermo Fisher Scientific) was diluted in Opti-MEM® I Reduced Serum Medium (ORSM) and mixed gently. Lipofectamine™ 2000 was also diluted with ORSM, mixed, and incubated for 15 minutes at room temperature (RT). After the incubation period, the siRNA solution was mixed with the Lipofectamine™ 2000 solution and incubated for 15 minutes at RT. Then, each well containing cells was treated with the siRNA-Lipofectamine™ 2000 mixture and mixed gently. Treated cells were incubated at 37°C and 5% CO<sub>2</sub> for 24 hours.

### ***Infections***

Prior to infection, viruses were diluted in a pre-warmed PBS/BSA mixture. Media was removed from the cells and the cells were washed with PBS. Virus dilutions were then added to each well and incubated for 1 hour at 37°C with periodic mixing. Then, the virus solution was removed from the cells and pre-warmed normal growth medium (RPMI+FBS) was added to each well. Cells were then incubated at 37°C and 5% CO<sub>2</sub> for up to 72 hours.

### *Western blots*

Western blots were used to confirm gene knockdown and to measure the clearance of viral protein (HA). Protein extraction for the western blots were conducted through a standard whole cell lysis protocol. Cells were washed with warm PBS and subsequently harvested with trypsin and warm media. Harvested cells were then centrifuged at 3,000 x g for 4 minutes. Cells were resuspended with cold PBS and mixed with 2x Laemmli sample buffer (Bio-Rad) and 10x NuPage Reducing Agent (Thermo Fisher). The cell solution was then heated at 95°C for 3 minutes to completely lyse the cells and reduce the proteins. Extracted cellular contents were stored at -20°C until use. To conduct the western blot, a gel and plastic blank was placed into the cassette and placed into an electrophoresis tank. The tank was filled with Running Buffer and wells were rinsed with Running Buffer to remove glycerol. Cellular extract samples and a Bio-Rad Plus Protein Dual Color Standard protein ladder were added into the wells, and unused wells were filled with Sample Buffer. The gels were run at 200 V for 0.5 hours. The gels were moved to a transfer cassette with a PVDF membrane pre-soaked in methanol, filter papers, and sponges, and placed in a clean tank filled with Transfer Buffer to run for 1 hour at 20V. After the transfer, the membranes were removed from the transfer cassette and blocked with a blocking buffer and rocked for 1 hour. Blocking solution was removed and diluted primary Ab (specific for each targeted gene) was added. The rabbit anti-HA primary antibody was purchased from Thermo Fisher Scientific. The mouse anti-actin primary antibody was purchased from ProteinTech. Membrane was rocked overnight at 4°C in the primary Ab solution. Primary Ab solution was removed and the membrane was washed 4 times for 4 minutes each with a wash buffer (10x PBS-T Wash Solution diluted 1:10 in distilled water) at RT. Membrane was then treated with

secondary Ab solution and subsequently rocked for 1.5 hours at RT. The secondary Abs (anti-mouse IR800, anti-rabbit IR700) were purchased from Azure Biosystems. Secondary Ab was removed and the membrane was washed 4 times for 4 minutes each with a wash buffer.

Membrane was then imaged using a digital imager.

## References

1. Histology, Respiratory Epithelium. In; 2021.
2. Acheson N. Fundamentals of Molecular Virology: John Wiley & Sons, Inc.; 2007.
3. Akram KM, Lomas NJ, Spiteri MA, Forsyth NR. Club cells inhibit alveolar epithelial wound repair via TRAIL-dependent apoptosis. *Eur Respir J* 2013; 41:683-94.
4. Ampomah PB, Lim LHK. Influenza A virus-induced apoptosis and virus propagation. *Apoptosis* 2020; 25:1-11.
5. Anastasina M, Le May N, Bugai A, Fu Y, Söderholm S, Gaelings L, et al. Influenza virus NS1 protein binds cellular DNA to block transcription of antiviral genes. *Biochim Biophys Acta* 2016; 1859:1440-8.
6. Atkinson JJ, Adair-Kirk TL, Kelley DG, Demello D, Senior RM. Clara cell adhesion and migration to extracellular matrix. *Respir Res* 2008; 9:1.
7. Boulo S, Akarsu H, Ruigrok RW, Baudin F. Nuclear traffic of influenza virus proteins and ribonucleoprotein complexes. *Virus Res* 2007; 124:12-21.
8. Bridge G, Rashid S, Martin SA. DNA mismatch repair and oxidative DNA damage: implications for cancer biology and treatment. *Cancers (Basel)* 2014; 6:1597-614.
9. Brincks EL, Gurung P, Langlois RA, Hemann EA, Legge KL, Griffith TS. The magnitude of the T cell response to a clinically significant dose of influenza virus is regulated by TRAIL. *J Immunol* 2011; 187:4581-8.

10. Chambers BS, Heaton BE, Rausch K, Dumm RE, Hamilton JR, Cherry S, et al. DNA mismatch repair is required for the host innate response and controls cellular fate after influenza virus infection. *Nat Microbiol* 2019; 4:1964-77.
11. Chen X, Liu S, Goraya MU, Maarouf M, Huang S, Chen JL. Host Immune Response to Influenza A Virus Infection. *Front Immunol* 2018; 9:320.
12. Chin KC, Cresswell P. Viperin (cig5), an IFN-inducible antiviral protein directly induced by human cytomegalovirus. *Proc Natl Acad Sci U S A* 2001; 98:15125-30.
13. Collins AR. The comet assay for DNA damage and repair: principles, applications, and limitations. *Mol Biotechnol* 2004; 26:249-61.
14. Downey J, Pernet E, Coulombe F, Divangahi M. Dissecting host cell death programs in the pathogenesis of influenza. *Microbes Infect* 2018; 20:560-9.
15. Drappier M, Michiels T. Inhibition of the OAS/RNase L pathway by viruses. *Curr Opin Virol* 2015; 15:19-26.
16. Dumm RE, Fiege JK, Waring BM, Kuo CT, Langlois RA, Heaton NS. Non-lytic clearance of influenza B virus from infected cells preserves epithelial barrier function. *Nat Commun* 2019; 10:779.
17. Dumm RE, Wellford SA, Moseman EA, Heaton NS. Heterogeneity of Antiviral Responses in the Upper Respiratory Tract Mediates Differential Non-lytic Clearance of Influenza Viruses. *Cell Rep* 2020; 32:108103.

18. Ehrhardt C, Wolff T, Pleschka S, Planz O, Beermann W, Bode JG, et al. Influenza A virus NS1 protein activates the PI3K/Akt pathway to mediate antiapoptotic signaling responses. *J Virol* 2007; 81:3058-67.
19. Gack MU, Albrecht RA, Urano T, Inn KS, Huang IC, Carnero E, et al. Influenza A virus NS1 targets the ubiquitin ligase TRIM25 to evade recognition by the host viral RNA sensor RIG-I. *Cell Host Microbe* 2009; 5:439-49.
20. Gomme EA, Wirblich C, Addya S, Rall GF, Schnell MJ. Immune clearance of attenuated rabies virus results in neuronal survival with altered gene expression. *PLoS Pathog* 2012; 8:e1002971.
21. Goraya MU, Zaighum F, Sajjad N, Anjum FR, Sakhawat I, Rahman SU. Web of interferon stimulated antiviral factors to control the influenza A viruses replication. *Microb Pathog* 2020; 139:103919.
22. Griffin DE. Recovery from viral encephalomyelitis: immune-mediated noncytolytic virus clearance from neurons. *Immunol Res* 2010; 47:123-33.
23. Guidotti LG, Borrow P, Brown A, McClary H, Koch R, Chisari FV. Noncytopathic clearance of lymphocytic choriomeningitis virus from the hepatocyte. *J Exp Med* 1999; 189:1555-64.
24. Guidotti LG, Ishikawa T, Hobbs MV, Matzke B, Schreiber R, Chisari FV. Intracellular inactivation of the hepatitis B virus by cytotoxic T lymphocytes. *Immunity* 1996; 4:25-36.

25. Guo G, Gao M, Gao X, Zhu B, Huang J, Tu X, et al. Reciprocal regulation of RIG-I and XRCC4 connects DNA repair with RIG-I immune signaling. *Nat Commun* 2021; 12:2187.
26. Guo Z, Chen LM, Zeng H, Gomez JA, Plowden J, Fujita T, et al. NS1 protein of influenza A virus inhibits the function of intracytoplasmic pathogen sensor, RIG-I. *Am J Respir Cell Mol Biol* 2007; 36:263-9.
27. Hao W, Wang L, Li S. Roles of the Non-Structural Proteins of Influenza A Virus. *Pathogens* 2020; 9.
28. Heaton NS, Langlois RA, Sachs D, Lim JK, Palese P, tenOever BR. Long-term survival of influenza virus infected club cells drives immunopathology. *J Exp Med* 2014; 211:1707-14.
29. Iyer RR, Pluciennik A, Burdett V, Modrich PL. DNA mismatch repair: functions and mechanisms. *Chem Rev* 2006; 106:302-23.
30. Javanian M, Barary M, Ghebrehewet S, Koppolu V, Vasigala V, Ebrahimpour S. A brief review of influenza virus infection. *J Med Virol* 2021; 93:4638-46.
31. Ji ZX, Wang XQ, Liu XF. NS1: A Key Protein in the "Game" Between Influenza A Virus and Host in Innate Immunity. *Front Cell Infect Microbiol* 2021; 11:670177.
32. Katze MG, He Y, Gale M. Viruses and interferon: a fight for supremacy. *Nat Rev Immunol* 2002; 2:675-87.
33. Killip MJ, Fodor E, Randall RE. Influenza virus activation of the interferon system. *Virus Res* 2015; 209:11-22.



34. Knipe D, Howley P. *Fields Virology*: Lippincott Williams & Wilkins; 2013.
35. Kuriakose T, Kanneganti TD. Regulation and functions of NLRP3 inflammasome during influenza virus infection. *Mol Immunol* 2017; 86:56-64.
36. Lenschow DJ, Lai C, Frias-Staheli N, Giannakopoulos NV, Lutz A, Wolff T, et al. IFN-stimulated gene 15 functions as a critical antiviral molecule against influenza, herpes, and Sindbis viruses. *Proc Natl Acad Sci U S A* 2007; 104:1371-6.
37. Li N, Parrish M, Chan TK, Yin L, Rai P, Yoshiyuki Y, et al. Influenza infection induces host DNA damage and dynamic DNA damage responses during tissue regeneration. *Cell Mol Life Sci* 2015; 72:2973-88.
38. Lin X, Wang R, Zou W, Sun X, Liu X, Zhao L, et al. The Influenza Virus H5N1 Infection Can Induce ROS Production for Viral Replication and Host Cell Death in A549 Cells Modulated by Human Cu/Zn Superoxide Dismutase (SOD1) Overexpression. *Viruses* 2016; 8.
39. Liu M, Chen F, Liu T, Liu S, Yang J. The role of oxidative stress in influenza virus infection. *Microbes Infect* 2017; 19:580-6.
40. Mathieu NA, Paparisto E, Barr SD, Spratt DE. HERC5 and the ISGylation Pathway: Critical Modulators of the Antiviral Immune Response. *Viruses* 2021; 13.
41. Min JY, Krug RM. The primary function of RNA binding by the influenza A virus NS1 protein in infected cells: Inhibiting the 2'-5' oligo (A) synthetase/RNase L pathway. *Proc Natl Acad Sci U S A* 2006; 103:7100-5.

42. Murphy K, Weaver C. Janeway's Immunobiology. 9 ed: Garland Science, Taylor & Francis Group, LLC; 2017.
43. Olive PL, Banáth JP. The comet assay: a method to measure DNA damage in individual cells. *Nat Protoc* 2006; 1:23-9.
44. Peteranderl C, Herold S. The Impact of the Interferon/TNF-Related Apoptosis-Inducing Ligand Signaling Axis on Disease Progression in Respiratory Viral Infection and Beyond. *Front Immunol* 2017; 8:313.
45. Piasecka J, Jarmolowicz A, Kierzek E. Organization of the Influenza A Virus Genomic RNA in the Viral Replication Cycle-Structure, Interactions, and Implications for the Emergence of New Strains. *Pathogens* 2020; 9.
46. Plotch SJ, Bouloy M, Krug RM. Transfer of 5'-terminal cap of globin mRNA to influenza viral complementary RNA during transcription in vitro. *Proc Natl Acad Sci U S A* 1979; 76:1618-22.
47. Rossman JS, Lamb RA. Influenza virus assembly and budding. *Virology* 2011; 411:229-36.
48. Sahu I, Glickman MH. Proteasome in action: substrate degradation by the 26S proteasome. *Biochem Soc Trans* 2021; 49:629-44.
49. Salomon JJ, Muchitsch VE, Gausterer JC, Schwagerus E, Huwer H, Daum N, et al. The cell line NCI-H441 is a useful in vitro model for transport studies of human distal lung epithelial barrier. *Mol Pharm* 2014; 11:995-1006.

50. Samji T. Influenza A: understanding the viral life cycle. *Yale J Biol Med* 2009; 82:153-9.
51. Sowa JN, Jiang H, Somasundaram L, Tecle E, Xu G, Wang D, et al. The *Caenorhabditis elegans* RIG-I Homolog DRH-1 Mediates the Intracellular Pathogen Response upon Viral Infection. *J Virol* 2020; 94.
52. Tang Y, Zhong G, Zhu L, Liu X, Shan Y, Feng H, et al. Herc5 attenuates influenza A virus by catalyzing ISGylation of viral NS1 protein. *J Immunol* 2010; 184:5777-90.
53. Tisoncik JR, Billharz R, Burmakina S, Belisle SE, Proll SC, Korth MJ, et al. The NS1 protein of influenza A virus suppresses interferon-regulated activation of antigen-presentation and immune-proteasome pathways. *J Gen Virol* 2011; 92:2093-104.
54. Uetani K, Hiroi M, Meguro T, Ogawa H, Kamisako T, Ohmori Y, et al. Influenza A virus abrogates IFN-gamma response in respiratory epithelial cells by disruption of the Jak/Stat pathway. *Eur J Immunol* 2008; 38:1559-73.
55. Wang L, Zhu S, Xu G, Feng J, Han T, Zhao F, et al. Gene Expression and Antiviral Activity of Interleukin-35 in Response to Influenza A Virus Infection. *J Biol Chem* 2016; 291:16863-76.
56. Wang X-x, Lu C, Rong E-g, Hu J-x, Xing Y-l, Liu Z-y, et al. Identification of novel genes associated with duck OASL in response to influenza A virus *Journal of Investigative Agriculture*, 2019:1451-9.

57. Wheeler DL, Athmer J, Meyerholz DK, Perlman S. Murine Olfactory Bulb Interneurons Survive Infection with a Neurotropic Coronavirus. *J Virol* 2017; 91.
58. Zhang J, Pavlova NN, Thompson CB. Cancer cell metabolism: the essential role of the nonessential amino acid, glutamine. *EMBO J* 2017; 36:1302-15.
59. Zhao C, Hsiang TY, Kuo RL, Krug RM. ISG15 conjugation system targets the viral NS1 protein in influenza A virus-infected cells. *Proc Natl Acad Sci U S A* 2010; 107:2253-8.
60. Zhao C, Zheng S, Zhu D, Lian X, Liu W, Hu F, et al. Identification of a novel porcine OASL variant exhibiting antiviral activity. *Virus Res* 2018; 244:199-207.
61. Zhu J, Zhang Y, Ghosh A, Cuevas RA, Forero A, Dhar J, et al. Antiviral activity of human OASL protein is mediated by enhancing signaling of the RIG-I RNA sensor. *Immunity* 2014; 40:936-48.